

# Robust measures of dispersion for circular data with an anomaly detection rule

Houyem Demni\*   Mia Hubert<sup>†</sup>   Giovanni C. Porzio<sup>‡</sup>   Peter J. Rousseeuw<sup>§</sup>

February 28, 2026

## Abstract

Circular variables that represent directions or periodic observations arise in many fields, such as biology and environmental sciences. An important issue when dealing with circular data is how to estimate their dispersion robustly, avoiding undue effects of anomalies. This work extends three robust dispersion measures from the line to the circle. Their robustness is studied via their influence functions and relative bias curves. From these dispersion measures, robust estimators of parameters of circular distributions can be derived. This yields robust estimators for the concentration parameter of the von Mises distribution and the dispersion parameter of the wrapped normal distribution. Their breakdown values and statistical efficiencies are obtained, and they are compared in a simulation study. Building on the best performing estimator, a robust circular anomaly detection procedure is developed, and employed to visualize outliers through a circular violin plot. Three real datasets are analyzed.

*Keywords:* Breakdown value, Circular Median Absolute Deviation, Circular Least Median Spread, Circular Least Trimmed Standard Deviation, Directional data, Outlier detection.

## 1 Introduction

In several application areas one may encounter circular data, consisting of angles, directions, and periodic observations that are represented as points on a circle. Circular data are found in biosciences with a broad range of interesting applications in several areas such as distributional models (Mardia et al., 2007), parametric and nonparametric estimation (Tishkovskaya and Blackwell, 2021), regression (Hassanzadeh, 2021) and clustering (Ranalli and Maruotti, 2020). See also Ley and Verdebout (2017, 2019) for a variety of modern methods and data examples. Because circular data lie on a bounded nonlinear manifold, specific statistical methods have been developed for their

---

\*Department of Economics and Law, University of Cassino and Southern Lazio, Italy, houyem.demni@unicas.it

<sup>†</sup>Section of Statistics and Data Science, KU Leuven, Leuven, Belgium, mia.hubert@kuleuven.be

<sup>‡</sup>Department of Economics and Law, University of Cassino and Southern Lazio, Italy, porzio@unicas.it

<sup>§</sup>Section of Statistics and Data Science, KU Leuven, Leuven, Belgium, peter@rousseeuw.net

analysis, see for instance [Buttarazzi et al. \(2018\)](#), [Fernández-Durán \(2007\)](#), and [Di Marzio et al. \(2022\)](#).

Standard measures of location and dispersion include the circular mean and the circular standard deviation CSD. Their precise definitions are given in Section 2. These measures are however very sensitive to outlying values. To illustrate this, we consider the directions in which 22 Sardinian sea stars traveled after displacement from their natural habitat ([Fisher, 1995](#)). The data are shown in Figure 1 and contain two unusual observations that we colored red. The CSD of the full data set is 0.58, but when the two special observations are removed it drops substantially, to 0.36.

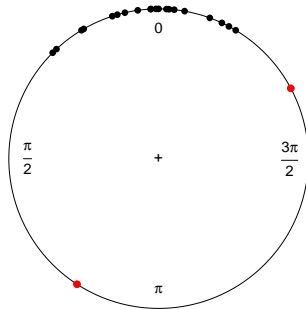


Figure 1: Circular plot of the directions traveled by Sardinian sea stars. Two unusual observations are colored red.

To deal with this sensitivity to anomalous values, we can employ robust measures instead. A robust measure of location for circular data is the *circular median*. It has been shown to possess well-established robustness properties in the family of unimodal symmetric distributions ([Ko and Guttorp, 1988](#)). The circular median is the same for the full sea stars dataset and without the two suspicious observations.

However, robust measures of circular dispersion have received less attention so far, unlike in the linear setting. A well-known robust dispersion estimator on the line is the median absolute deviation (MAD), described by [Hampel et al. \(1986\)](#) and [Leys et al. \(2013\)](#). A circular version called CMAD has been used to compare the performance of some circular location estimators ([Otieno and Anderson-Cook, 2006](#)), to lower a false alarm rate in the detection of transiting planets ([Seader et al., 2013](#)), and to obtain a smoothing parameter when nonparametrically estimating the off-pulse interval of a pulsar light curve ([Schutte and Swanepoel, 2016](#)).

In spite of this, the CMAD has not yet been studied by the tools of robust statistics such as the influence function and the breakdown value. We will do so in this paper. We will also study the circular counterparts of two other robust measures of scale for linear data, the least median squares (LMS) and least trimmed squares (LTS) methods, that were first proposed by [Rousseeuw \(1984\)](#) in a regression setting. The resulting CLMS and CLTS methods will be defined and compared with

CMAD.

We will also use these dispersion measures to derive robust estimators for the dispersion parameters of standard circular distributions. We will provide a detailed treatment of the estimation of the concentration parameter  $\kappa$  of the von Mises distribution, and of the dispersion parameter  $\sigma$  of the wrapped normal distribution.

Finally, we construct an outlier detection rule on the circle based on our results, and introduce a companion graphical tool that is a variation on the well-known violin plot.

The paper is organized as follows. Section 2 reviews a few background concepts of circular data. The CMAD, CLMS and CLTS measures are defined in Section 3. Their influence functions are derived in Section 4, and their relative bias under contamination is computed in Section 5. Section 6 constructs corresponding estimators for dispersion parameters of circular distributions, provides their breakdown values, and studies their efficiency. Section 7 introduces a robust anomaly detection rule and the circular violin plot. Section 8 analyzes three real data examples, and Section 9 concludes.

## 2 Background material

Circular data consists of points on the unit circle. The same point can be either defined in polar coordinates by an angle  $\theta \in [-\pi, \pi)$  measured in radians, once an origin and an orientation have been chosen, or in Cartesian coordinates as a vector  $x = (x_1, x_2)^T = (\cos \theta, \sin \theta)^T$  so  $x \in \mathcal{S} := \{x : \|x\| = 1\}$ . Back-transformation is obtained through  $\theta = \arctan2(x_2, x_1)$ .

Note that the angles  $\theta$  and  $\theta + 2\pi$  yield the same point on the circle. The arithmetic for circular data is therefore modulo  $2\pi$ , and for the sake of simplicity we will write  $\theta_1 + \theta_2$  instead of  $\theta_1 + \theta_2 \bmod 2\pi$  where  $\theta_1$  and  $\theta_2$  are two points on the circle.

The notation based on angles is more economical than the notation with Cartesian coordinates, so we will mostly use angles. A circular random variable can be denoted as  $\Theta$ , and its distribution function as  $F(\theta) = P(\Theta \leq \theta)$  for  $\theta \in [-\pi, \pi)$ .

Throughout this work we will repeatedly use the length of the shortest arc joining two points on the unit circle, that we denote as the shortest arc distance  $d(\theta_1, \theta_2) := \pi - |\pi - |\theta_1 - \theta_2||$ .

### 2.1 Location and dispersion of circular random variables

The location of a circular random variable is often measured by its circular mean. Let  $\Theta$  be a circular random variable with distribution  $F$ . Its circular mean is defined as the angle  $\mu(F) = \arctan2(\beta_1, \alpha_1)$  with

$$\alpha_1 = \mathbb{E}(\cos \Theta) = \int_{-\pi}^{\pi} \cos \theta dF(\theta) \quad \text{and} \quad \beta_1 = \mathbb{E}(\sin \Theta) = \int_{-\pi}^{\pi} \sin \theta dF(\theta).$$

The *circular median set* of  $\Theta$  is instead defined as the set of points that minimize the mean angular distance.

**Definition 1** (Circular Median Set). The circular median set  $M_\Theta$  of a random variable  $\Theta$  is defined as:

$$M_\Theta := \{\theta : \arg \min_{\theta} \mathbb{E}(d(\Theta, \theta))\}, \quad \theta \in [-\pi, \pi) \quad (1)$$

where  $\mathbb{E}(T)$  is the expected value of the (linear) random variable  $T$ .

Any element in  $M_\Theta$  is called a *circular median* or Fréchet median. The circular median set can be a singleton, the whole circle (for instance, at the uniform distribution) or even a disconnected set. Circular random variables with unique median do exist. For instance, if a distribution admits a continuous density and it is unimodal, then its circular median is unique (Mardia, 1972). If  $\Theta$  has a unique circular median, we denote it as  $\tilde{\mu}$ .

**Definition 2** (Circular Variance). The circular variance of a random variable  $\Theta$  is given by

$$\text{CV}(F) = 2(1 - \rho) = \int_{-\pi}^{\pi} 2(1 - \cos(\theta - \mu)) dF(\theta) \quad (2)$$

where  $\mu$  is the circular mean of  $\Theta$  and

$$\rho = \left| \int_{-\pi}^{\pi} e^{i\theta} dF(\theta) \right| = \int_{-\pi}^{\pi} \cos(\theta - \mu) dF(\theta) \quad (3)$$

is the mean resultant length.

Both the circular variance and the mean resultant length are bounded, with  $0 \leq \text{CV}(F) \leq 2$  and  $0 \leq \rho \leq 1$ . Some authors drop the factor 2 in (2), but we prefer this version because for increasing concentration, when the distribution is concentrated on a small near-linear part of the circle, (2) corresponds to the linear variance. This is because the leading term of the Taylor expansion of  $2(1 - \cos(\theta - \mu))$  for  $\theta$  around  $\mu$  is  $(\theta - \mu)^2$ , see also page 21 of Jammalamadaka and Sengupta (2001). Here we will mainly work with the square root of (2), which is the *circular standard deviation* denoted by

$$\text{CSD}(F) = \sqrt{\text{CV}(F)}.$$

A measure on the circle is said to be rotationally invariant if it is unchanged under all rotations. A measure is equivariant under rotations if rotating the circle rotates the measure in the same way. A circular distribution  $F$  is said to be reflectionally symmetric about a direction  $\mu$  if its probability function is such that  $P(\Theta \in (\mu - \theta, \mu)) = P(\Theta \in (\mu, \mu + \theta))$  for all  $\theta \in [-\pi, \pi)$ .

If a circular distribution  $F$  admits a density  $f$ , it is said to be rotationally symmetric of order  $m$ , with  $m \in \mathbb{N}$ , if the density repeats every  $2\pi/m$  radians, that is,  $f(\theta) = f(\theta + 2\pi/m)$  for all  $\theta$ . It is said to be antipodally symmetric if  $f(\theta) = f(\theta + \pi)$  for all  $\theta \in [-\pi, \pi)$ , that is, if the density is invariant under a rotation of  $\pi$  radians. Moreover, the distribution is monotone reflectionally symmetric about  $\mu$  if it is reflectionally symmetric and  $f(\mu + \theta)$  is non-increasing for  $\theta \in [0, \pi]$ , so that the density attains its maximum at  $\mu$  and decreases symmetrically in both directions.

## 2.2 The von Mises and wrapped normal distributions

The von Mises distribution  $vM(\mu, \kappa)$  is the most often used distribution to model circular data, and sometimes called the circular normal distribution. Its density is given by

$$f_{vM}(\theta; \mu, \kappa) := \frac{1}{2\pi I_0(\kappa)} \exp(\kappa \cos(\theta - \mu)),$$

with  $I_0$  the modified Bessel function of the first kind and order 0. Here  $\mu \in [-\pi, \pi)$  is the location parameter and  $\kappa \geq 0$  is the concentration parameter. The location parameter  $\mu$  is simultaneously the circular mean, the mode and the circular median. The density has a shape resembling the normal distribution, and it approaches the normal distribution as its concentration  $\kappa$  gets higher. For  $\kappa = 0$ , the distribution reduces to the continuous uniform distribution on the circle. For  $\kappa > 0$ , the distribution is unimodal and reflectionally symmetric around  $\mu$ . The concentration parameter  $\kappa$  and the circular variance are related through the mean resultant length  $\rho = I_1(\kappa)/I_0(\kappa)$  with  $I_1$  the modified Bessel function of the first kind of order 1. Consequently,  $\kappa$  is implicitly defined as the solution of  $I_1(\kappa)/I_0(\kappa) = 1 - \text{CSD}^2/2$ , which admits no analytic expression and must be evaluated numerically.

Another widely used reflectionally symmetric distribution for unimodal circular data is the wrapped normal distribution  $WN(\mu, \sigma^2)$  with density

$$f_{WN}(\theta; \mu, \sigma^2) := \frac{1}{\sigma\sqrt{2\pi}} \sum_{m=-\infty}^{\infty} \exp\left(\frac{-(\theta - \mu + 2\pi m)^2}{2\sigma^2}\right).$$

Its location parameter is  $\mu \in [-\pi, \pi)$ , and  $0 < \sigma^2 < +\infty$  is the variance of the linear normal distribution that gets wrapped around the circle. The mean resultant length of the wrapped normal distribution is  $\rho = \exp(-\sigma^2/2)$ , which decreases as  $\sigma^2$  increases. The CSD is directly related to  $\sigma^2$  by  $\text{CSD}^2 = 2(1 - \exp(-\sigma^2/2))$ .

## 3 Three measures of circular dispersion

In this section we define the Circular Median Absolute Deviation (CMAD), the Circular Least Median Spread (CLMS), and the Circular Least Trimmed Standard Deviation (CLTS).

### 3.1 The Circular Median Absolute Deviation (CMAD)

The CMAD is defined for distributions  $F$  with a unique circular median and equals the (linear) median of the distribution of the shortest arc distances from this (circular) median.

**Definition 3** (CMAD). Let  $\mathcal{M}_1$  be the set of circular random variables whose unique circular median is  $\tilde{\mu}$ . The CMAD of  $\Theta \in \mathcal{M}_1$  is given by:

$$\text{CMAD}(F) := \text{Median}(d(\Theta, \tilde{\mu})) \tag{4}$$

where  $\text{Median}(T)$  refers to the median of the (linear) random variable  $T$ . That is,  $\text{Median}(T)$  is the set of values  $x$  such that  $P(T \leq x) \geq 0.5$  and  $P(T \geq x) \geq 0.5$ . If such a set is an interval, its midpoint is taken as the median value.

For circular random variables admitting a density,  $\text{CMAD}(F)$  is half the length of the shortest arc that is symmetric around  $\tilde{\mu}$  and encompasses probability 0.5:

$$\begin{aligned} \text{CMAD}(F) &= \frac{1}{2} d(\theta_1, \theta_2), \\ \{\theta_1, \theta_2\} &= \arg \min_{\theta_1, \theta_2 \in [-\pi, \pi]} \{d(\theta_1, \theta_2) \mid P(\theta_1 \leq \Theta \leq \theta_2) = 0.5, d(\theta_1, \tilde{\mu}) = d(\theta_2, \tilde{\mu})\} \end{aligned} \quad (5)$$

The Circular Median Absolute Deviation (CMAD) is nonnegative. It is rotational invariant because the circular median is rotational equivariant and the shortest arc distances are rotational invariant. It is also reflectionally invariant because the circular median is equivariant under reflection, while the shortest arc distances are invariant.

CMAD is a bounded measure of circular dispersion that satisfies  $0 \leq \text{CMAD}(F) < \pi$ . We now investigate the range that CMAD can take, depending on the distribution. The proof of the next lemma, as well as the proofs of all other theoretical results, is deferred to the Supplementary Material.

**Lemma 1** (Values of CMAD). *Let  $\Theta \in \mathcal{M}_1$  be a circular random variable, and  $\theta \in [-\pi, \pi)$ .*

$$\begin{aligned} \text{If } \exists \theta : P(\Theta = \theta) > 0.5, & \quad \text{then } \text{CMAD}(F) = 0; \\ \text{If } \exists \theta : P(\Theta = \theta) = 0.5, & \quad \text{then } 0 \leq \text{CMAD}(F) < \pi/2; \\ \text{If } \forall \theta : P(\Theta = \theta) < 0.5, & \quad \text{then } 0 < \text{CMAD}(F) < \pi. \end{aligned}$$

By Lemma 1,  $\pi$  is an upper bound for CMAD. The following result shows that this bound is sharp.

**Theorem 1.** *For  $F$  ranging over the set of cdf's of all circular random variables,  $\sup_F \text{CMAD}(F) = \pi$ .*

For reflectionally symmetric distributions, the value of CMAD is a quantile of the distribution itself. The following result follows directly from Equation (5).

**Theorem 2** (Value of CMAD under reflectional symmetry). *Let  $\Theta \in \mathcal{M}_1$  be reflectionally symmetric about some  $\mu^*$ . Then the circular median of  $\Theta$  is either  $\mu^*$  or  $\mu^* + \pi$ . If  $\mu^*$ ,  $\text{CMAD}(F)$  equals the length of the shortest arc joining  $\mu^*$  with the point  $\xi$  cumulating 25% of probability from  $\mu^*$  itself, either clockwise or counterclockwise. That is, with*

$$\xi : \int_{\mu^*}^{\xi} dF(\theta) = 0.25, \quad (6)$$

we have:

$$\text{CMAD}(F) = d(\xi, \mu^*). \quad (7)$$

If the circular median of  $\Theta$  is  $\mu^* + \pi$ , Equations (6) and (7) apply to  $\mu^* + \pi$ .

The CMAD is not defined when the circular median is not unique. For this reason we define two other dispersion measures that do not depend on the circular median.

### 3.2 The Circular Least Median Spread (CLMS)

The Circular Least Median Spread (CLMS) extends the Least Median Squares dispersion measure (Rousseeuw, 1984; Rousseeuw and Leroy, 1987) from the line to the circle. The CLMS is the smallest median distance of the random variable to a point on the circle.

**Definition 4** (CLMS). Let  $\Theta$  be a circular random variable with distribution  $F$ , and  $\theta$  ranges over all points on the circle. Then the CLMS is given by:

$$\text{CLMS}(F) := \min_{\theta} \text{Median}(d(\Theta, \theta)).$$

Equivalently, CLMS is half the length of the shortest arc that encompasses at least half of the probability distribution:

$$\text{CLMS}(F) = \frac{1}{2} \min\{d(\theta_1, \theta_2) | P(\theta_1 \leq \Theta \leq \theta_2) \geq 0.5\}, \quad (8)$$

where  $\theta_1$  and  $\theta_2$  are two points on the circle. The CLMS is nonnegative, and invariant under rotation and reflection. We now study the conditions under which the CLMS reaches its minimum and maximum attainable value.

**Lemma 2** (Conditions for CLMS = 0). *Let  $\Theta$  be a circular random variable with distribution  $F$ , and  $\Delta_{\theta}$  denote the point mass circular distribution in  $\theta$ . We have:*

$$\text{CLMS}(F) = 0 \quad \text{iff} \quad F = (1 - \varepsilon)\Delta_{\theta} + \varepsilon G, \quad 0 \leq \varepsilon \leq 0.5,$$

for any value  $\theta$  and any distribution  $G$ .

**Lemma 3** (Maximum of CLMS). *Let  $\Theta \in [-\pi, \pi)$  be a circular random variable with distribution  $F$ . Then,*

$$\max_F \text{CLMS}(F) = \pi/2.$$

The result holds because  $\text{CLMS}(F)$  cannot be larger than  $\pi/2$ , since  $\pi$  is the maximal length of the shortest path connecting two points on a circle. On the other hand,  $\text{CLMS} = \pi/2$  characterizes a class of distributions, as seen in the following theorem.

**Theorem 3.** *Let  $\Theta$  be a circular random variable with distribution  $F$ . Then*

$$\text{CLMS}(F) = \pi/2 \quad \Leftrightarrow \quad F \in H_{0.5}$$

where  $H_{0.5}$  is the class of distributions that satisfy  $\int_{HC} dH_{0.5}(\theta) = 0.5$  for any semicircle  $HC$ .

The class  $H_{0.5}$  is a subset of the class of the centrally (or antipodal) symmetric distributions  $H$ , because they satisfy  $\int_{HC} dH(\theta) \geq 0.5$  for any semicircle  $HC$ , see e.g. the discussion in [Nagy et al. \(2024\)](#).

Note that the CSD has a similar implication to the  $\Leftarrow$  in Theorem 3. Because distributions in  $H_{0.5}$  have antipodal symmetry their resultant length is 0, so their CSD takes the maximal value  $\sqrt{2}$ . But the  $\Rightarrow$  does not hold. For instance, a rotationally symmetric distribution  $F$  of order  $m = 3$  has  $\text{CSD}(F) = \sqrt{2}$ , but it does not belong to  $H_{0.5}$ .

A second remark contrasts CLMS with CMAD. By definition, the latter is not defined under  $H_{0.5}$  since those distributions do not have a unique circular median.

On the other hand, CLMS takes the same value as CMAD under monotone rotational symmetry, as stated below.

**Theorem 4.** *Let  $\Theta$  be a continuous circular random variable whose distribution  $F$  admits a density  $f$  that is reflectively symmetric about some  $\mu^*$  and strictly unimodal with mode  $\mu^*$ . Let  $\xi$  be the point cumulating 25% of probability from  $\mu$  itself, as in (6). Then*

$$\text{CLMS}(F) = d(\xi, \mu^*).$$

The theorem holds because the shortest arc is symmetric about the modal direction  $\mu^*$ . Moreover, by the continuity and the probability constraint in Equation (8), half of its length has a probability mass of 0.25. Note that monotone reflectional symmetry is a special case of reflectional symmetry, under which condition the same value was obtained for CMAD in Theorem 2.

### 3.3 The Circular Least Trimmed Standard deviation (CLTS)

The third robust measure of dispersion we discuss is the Circular Least Trimmed Standard deviation CLTS, which extends the least trimmed squares (LTS) dispersion ([Rousseeuw, 1984](#)) from the line to the circle. The CLTS is given by the smallest CSD over arcs that encompass at least 50% of probability mass.

For any  $\theta_1$  and  $\theta_2$ , and any circular random variable  $\Theta$  with distribution  $F$ , denote by  $F_{[\theta_1, \theta_2]}$  the conditional distribution of  $\Theta$  given  $\theta_1 \leq \Theta \leq \theta_2$  and  $\mu_{[\theta_1, \theta_2]}$  its circular mean.

**Definition 5 (CLTS).** Let  $\Theta$  be a circular random variable with distribution  $F$ . Then the Circular Least Trimmed Standard deviation (CLTS) is defined as

$$\text{CLTS}(F) := \min_{\theta_1, \theta_2} \{\text{CSD}(F_{[\theta_1, \theta_2]}) \mid P(\theta_1 \leq \Theta \leq \theta_2) \geq 0.5\}. \quad (9)$$

The CLTS is nonnegative, rotational and reflective invariant because the CSD is. From (2) it follows that

$$\text{CLTS}(F) := \min_{\theta_1, \theta_2} \left\{ \sqrt{\frac{\int_{\theta_1}^{\theta_2} 2(1 - \cos(\theta - \mu_{[\theta_1, \theta_2]}))dF(\theta)}{P(\theta_1 \leq \Theta \leq \theta_2)}} \mid P(\theta_1 \leq \Theta \leq \theta_2) \geq 0.5 \right\}. \quad (10)$$

**Lemma 4** (Conditions for CLTS = 0). *Let  $\Theta$  be a circular random variable with distribution  $F$ , and  $\Delta_\theta$  be the point mass in some  $\theta$ . Then*

$$\text{CLTS}(F) = 0 \quad \Leftrightarrow \quad F = (1 - \varepsilon)\Delta_\theta + \varepsilon G, \quad 0 \leq \varepsilon \leq 0.5,$$

for any value  $\theta$  and any distribution  $G$ .

For the maximal value of CLTS, we can rely on the following result.

**Lemma 5.** *Let  $F$  be the continuous circular uniform distribution. That is,  $F$  has density  $1/(2\pi)$ . Then*

$$\text{CLTS}(F) = \sqrt{2(1 - 2/\pi)}.$$

The result can be derived from (10), because each semicircle contains exactly 0.5 of the probability mass. We conjecture that there is no other circular distribution (either discrete or continuous) whose CLTS attains this value.

Finally, it is possible to derive a general equation for the CLTS in the case of monotone reflective symmetry.

**Theorem 5.** *Let  $\Theta$  be a continuous circular random variable whose distribution  $F$  admits a density  $f$  that is reflectively symmetric about some  $\mu^*$  and strictly unimodal with mode  $\mu^*$ . Let  $\xi$  be the point that cumulates 25% of probability from  $\mu^*$  as in (6). Then*

$$\text{CLTS}(F) = \sqrt{4 \int_{\mu^*}^{\mu^* + \xi} 2(1 - \cos(\theta - \mu^*))dF(\theta)}. \quad (11)$$

This holds by (10) and because the conditional distribution with minimal CSD is reflectively symmetric about  $\mu^*$ .

### 3.4 Values, infimum, and supremum at von Mises and wrapped normal

**Corollary 1.** *Let  $F = vM(\mu, \kappa > 0)$  or  $F = WN(\mu, \sigma^2)$  and denote  $q_1 = F^{-1}(1/4)$  and  $q_3 = F^{-1}(3/4)$ . Then*

$$\text{CMAD}(F) = \text{CLMS}(F) = q_3 - \mu \quad (12)$$

$$\text{CLTS}(F) = \text{CSD}(F_{[q_1, q_3]}) \quad (13)$$

This follows from Theorems 2, 4 and 5. The infimum and the supremum of CMAD, CLMS, CLTS at a von Mises distribution with  $\kappa > 0$  and at the wrapped normal are given below.

**Corollary 2.** *Let  $\Theta \sim vM(\mu, \kappa > 0)$  or  $\Theta \sim WN(\mu, \sigma^2)$ . Then*

$$\begin{aligned} \inf \text{CMAD}(F) &= \inf \text{CLMS}(F) = \inf \text{CLTS}(F) = 0 \\ \sup \text{CMAD}(F) &= \sup \text{CLMS}(F) = \pi/2 \\ \sup \text{CLTS}(F) &= \sqrt{2(1 - 2/\pi)}. \end{aligned}$$

At the von Mises distribution, the infimum holds because of Lemma 1, Lemma 2, and Lemma 4, and because  $F \xrightarrow{d} \Delta_\mu$  for  $\kappa \rightarrow +\infty$ . The supremum follows from (12) and Lemma 5. It holds that  $\lim_{\kappa \rightarrow 0} \text{CMAD}(F) = \lim_{\kappa \rightarrow 0} \text{CLMS}(F) = \frac{\pi}{2}$  and  $\lim_{\kappa \rightarrow 0} \text{CLTS}(F) = \sqrt{2(1 - 2/\pi)}$ .

At the wrapped normal distribution we have  $\lim_{\sigma \rightarrow 0} \text{CMAD}(F) = \lim_{\sigma \rightarrow 0} \text{CLMS}(F) = \lim_{\sigma \rightarrow 0} \text{CLTS}(F) = 0$  because for  $\sigma \rightarrow 0$  the distribution becomes increasingly concentrated around  $\mu^*$ . We also have  $\lim_{\sigma \rightarrow +\infty} \text{CMAD}(F) = \lim_{\sigma \rightarrow +\infty} \text{CLMS}(F) = \frac{\pi}{2}$ , and  $\lim_{\sigma \rightarrow +\infty} \text{CLTS}(F) = \sqrt{2(1 - 2/\pi)}$ , because for  $\sigma \rightarrow +\infty$  the distribution approaches the uniform distribution.

## 4 Influence functions

The robustness of a functional can be measured in different ways. First, we consider its influence function which evaluates the effect of a small fraction of contamination. Formally, the influence function (Hampel et al., 1986) of a functional  $S$  in a point  $\theta$  at a model distribution  $F$  is defined as

$$\text{IF}(\theta; S, F) := \left. \frac{\partial}{\partial \varepsilon} S((1 - \varepsilon)F + \varepsilon\Delta_\theta) \right|_{\varepsilon=0+} = \lim_{\varepsilon \downarrow 0} \frac{S((1 - \varepsilon)F + \varepsilon\Delta_\theta) - S(F)}{\varepsilon}. \quad (14)$$

The influence function of CSD has been provided in Ko and Guttorp (1988) and is given by

$$\text{IF}(\theta; \text{CSD}, F) = \frac{1}{\text{CSD}(F)} \left( 1 - \frac{\text{CSD}^2(F)}{2} - \cos(\theta) \right)$$

for  $-\pi \leq \theta \leq \pi$ , and  $F$  a reflectively symmetric circular distribution with mode 0. We will now compute the influence functions of the CMAD, CLMS, and CLTS functionals. In order to deal with contaminated distributions like  $(1 - \varepsilon)F + \varepsilon\Delta_\theta$  we will consider distributions of the type

$$P = a_0 P_0 + \sum_{j=1}^k a_j \Delta_{\theta_j} \quad (15)$$

where  $a_0 > 0$ ,  $P_0$  is a distribution with continuous density  $f$  on the circle,  $k < \infty$ , all  $a_j > 0$ , all  $\theta_j$  in the interval  $] -\pi, \pi]$ , and  $\Delta_\theta$  the probability distribution that puts all its mass in the point  $\theta$ . Since  $P$  is a probability it must hold that  $a_0 + a_1 + \dots + a_k = 1$ . We then define the cumulative

distribution function  $G$  by  $G(\theta) = \int_{-\pi}^{\theta} g(u)du$  for  $-\pi \leq \theta \leq \pi$ . We thus have  $G(-\pi) = 0$  and  $G(\pi) = 1$ . We then extend  $G$  to the interval  $[-2\pi, 2\pi]$  by  $G(\theta) = G(\theta + 2\pi) - 1$  for  $-2\pi \leq \theta < -\pi$  and  $G(\theta) = G(\theta - 2\pi) + 1$  for  $\pi < \theta \leq 2\pi$ .  $G$  is right continuous so we can define  $G^{-1}$  in the usual way.

For any distribution function of the type (15) we can now write the functional CLMS( $G$ ) as

$$\text{CLMS}(G) = \frac{1}{2} \inf \left\{ G^{-1}\left(t + \frac{1}{2}\right) - G^{-1}(t) ; G(0) - 1 < t \leq G(0) + \frac{1}{2} \right\}. \quad (16)$$

**Theorem 6** (IF of CMAD and CLMS). *Let  $F$  be a circular distribution with continuous density  $f(\theta) > 0$  that is reflectively symmetric about 0 and strictly unimodal with mode 0 (i.e.,  $f$  is strictly decreasing on  $[0, \pi]$ ). Then the influence functions of both CMAD and CLMS are given by*

$$\text{IF}(\theta; S, F) = \frac{\text{sign}(|\theta| - F^{-1}(3/4))}{4f(F^{-1}(3/4))} \quad (17)$$

for  $-\pi \leq \theta \leq \pi$ , where  $\text{CMAD}(F) = \text{CLMS}(F) = F^{-1}(3/4)$  (by Theorems 2 and 4).

See Appendix B for the proof. Note that the conditions on  $F$  are satisfied by most of the classic models of circular statistics, including any von Mises distribution (with  $\mu = 0$  and  $\kappa > 0$ ) and any wrapped normal distribution (with  $\mu = 0$ ). It is interesting that CMAD and CLMS have the same influence function at such distributions  $F$ , even though they are quite different estimators.

Figure 2 shows the IF of CMAD and CLMS for a von Mises distribution with  $\mu = 0$  and  $\kappa = 1/2$ . Outside the interval  $[-\pi, \pi]$  it continues with period  $2\pi$ .

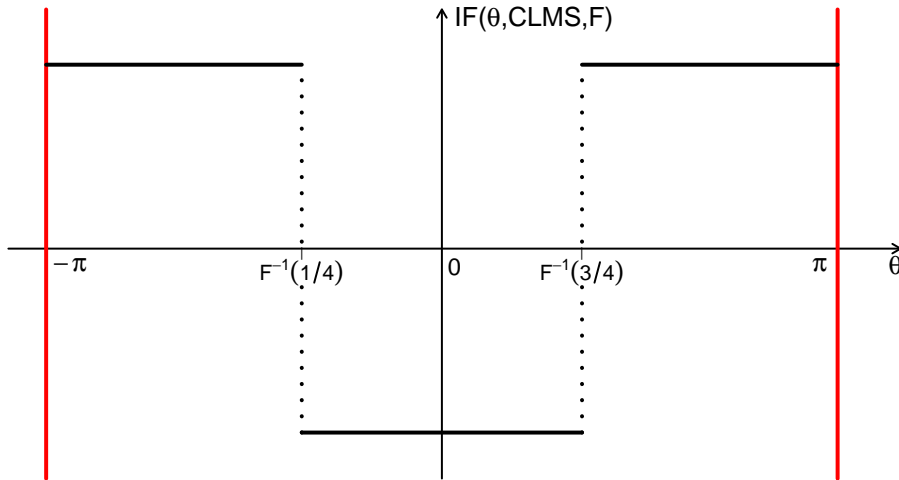


Figure 2: Influence function of CMAD and CLMS at the von Mises distribution with  $\mu = 0$  and  $\kappa = 1/2$ .

We see that the IF is a piecewise constant function which takes on the value  $1/(4f(F^{-1}(3/4)))$  for points outside the interval that determines the scale for the uncontaminated distribution  $F$ ,

and the opposite value when it lies inside that interval. This means that the standardized effect of a single point is quite small. When we add a point outside the interval CMAD and CLMS only go up a little bit, and when we put it inside they only go down a little bit. The size of the effect is measured by the so-called *gross-error-sensitivity* given by

$$\gamma^*(S, F) = \sup_{\theta} |\text{IF}(\theta; S, F)|$$

so  $\gamma^*(\text{CMAD}, F) = 1/(4f(F^{-1}(3/4))) = \gamma^*(\text{CLMS}, F)$ . The influence function of CLTS looks different.

**Theorem 7** (IF of CLTS). *Let  $F$  be a circular distribution with continuous density  $f(\theta) > 0$  that is reflectively symmetric about 0 and strictly unimodal with mode 0, that is,  $f$  is strictly decreasing on  $[0, \pi]$ . Then the influence function of the CLTS estimator  $S$  is given on  $[-\pi, \pi]$  by*

$$\begin{aligned} \text{IF}(\theta; S, F) = \frac{1}{S(F)} \left[ 1 - \frac{S^2(F)}{2} - \cos(F^{-1}(3/4)) \right. \\ \left. + 2I(|\theta| < F^{-1}(3/4)) (\cos(F^{-1}(3/4)) - \cos(\theta)) \right]. \end{aligned} \quad (18)$$

Figure 3 shows the IF of CLTS at the von Mises distribution with  $\mu = 0$  and  $\kappa = 1/2$ . Note that the central part of the IF has the shape of  $-\cos(\theta)$  whereas the IF of the LTS scale estimator in the linear setting is quadratic in the center (Croux and Rousseeuw, 1992). However, when the von Mises distribution gets more concentrated ( $\kappa \rightarrow \infty$ ) the IF of CLTS becomes indistinguishable from that of the linear LTS at a Gaussian distribution, since the Taylor expansion of  $-\cos(\theta)$  around zero is  $-1 + \theta^2/2 + o(\theta^3)$ . Also the IF's of CMAD and CLMS become indistinguishable from those of the scale estimators MAD and LMS in the linear setting.

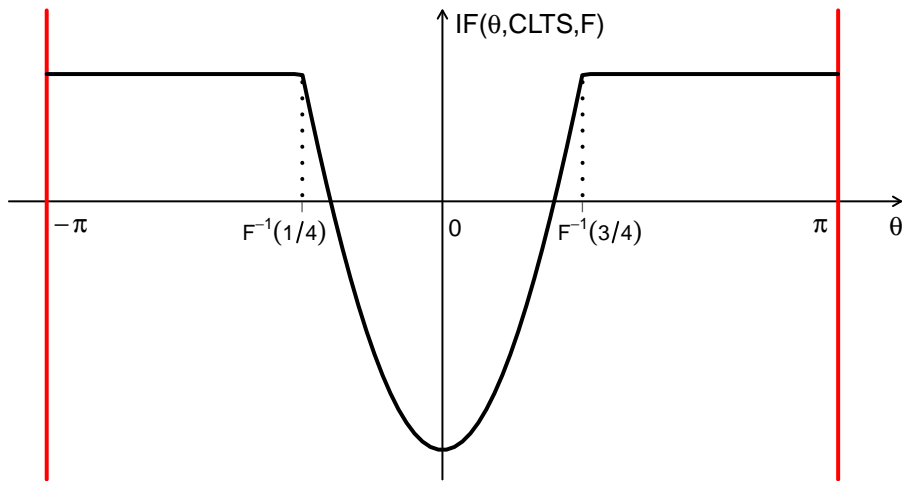


Figure 3: Influence function of CLTS at the von Mises distribution with  $\mu = 0$  and  $\kappa = 1/2$ .

Note that Theorems 6 and 7 give the influence functions of the ‘raw’ versions of CMAD, CLMS, and CLTS. In the sequel, we will consider transformations  $\zeta$  to make them consistent estimators of a parameter in a parametric model, so the actual estimators will be of the form  $\zeta(S)$  where  $S$  is the raw estimator. In that situation, we can compute the IF of the final estimator by the chain rule:

$$\text{IF}(\theta; \zeta(S), F) = \left. \frac{\partial}{\partial \varepsilon} \zeta \left( S((1 - \varepsilon)F + \varepsilon \Delta_\theta) \right) \right|_{\varepsilon=0+} = \zeta'(S(F)) \text{IF}(\theta; S, F), \quad (19)$$

so it is proportional to the IF of the raw estimator.

## 5 Bias curves

Whereas the influence function measures the effect of a very small proportion of point contamination on a functional, we can also study the impact of other types and sizes of contamination.

Here we consider von Mises distributions  $F$  and contaminating distributions  $G_{\theta, \varepsilon} = (1 - \varepsilon)F + \varepsilon \Delta_\theta$  for  $\theta \in [-\pi, \pi)$  and  $0 \leq \varepsilon < 0.5$ . We use point contamination because it often has the biggest effect on scale functionals (Martin and Zamar, 1989; Croux and Haesbroeck, 2001). We define the *relative bias* in  $\theta$  as

$$rb(\theta; S, F, \varepsilon) := \frac{S(G_{\theta, \varepsilon}) - S(F)}{S(F)} \quad (20)$$

where  $S$  is the CSD, CMAD, CLMS or CLTS functional. The denominator in (20) makes the values for the different functionals more comparable. Plotting the relative bias over the whole range of  $\theta$  values yields the *relative bias curve*.

To approximate these bias curves, we compute them on samples of size 5000. The sample versions of all the dispersion measures are computed using functions implemented in R. The sample CMAD is obtained by considering the empirical counterpart of Equation (4) and is computed with the R package `circular` (Lund and Agostinelli, 2013). According to (8), the sample CLMS is given by half the length of the shortest arc encompassing  $h = \lceil n/2 \rceil + 1$  sample points, where  $\lceil \cdot \rceil$  is the ceiling function. To obtain the sample CLTS we compute the CSD of all contiguous subsamples of size  $h = \lceil n/2 \rceil + 1$ , and keep the lowest CSD.

Figure 4 shows the relative bias curves at von Mises distributions  $F$  with location  $\mu = 0$  and concentration  $\kappa \in \{2, 5\}$ . In each scenario, the contamination level was set to  $\varepsilon \in \{5\%, 10\%, 20\%\}$ .

We see that the bias curves of the dispersion measures have a shape that resembles their influence functions. When the contamination is located in the central part of the distribution, the bias is negative. Outside that region the bias is positive. The effect becomes larger with increasing contamination. The impact of the contamination on the circular standard deviation CSD is much larger than the effect on CMAD, CLMS and CLTS. Among the three robust estimators, CMAD shows the largest positive bias in the outer part of the distribution whereas CLTS has the largest negative bias in the central part, but the differences are slight.

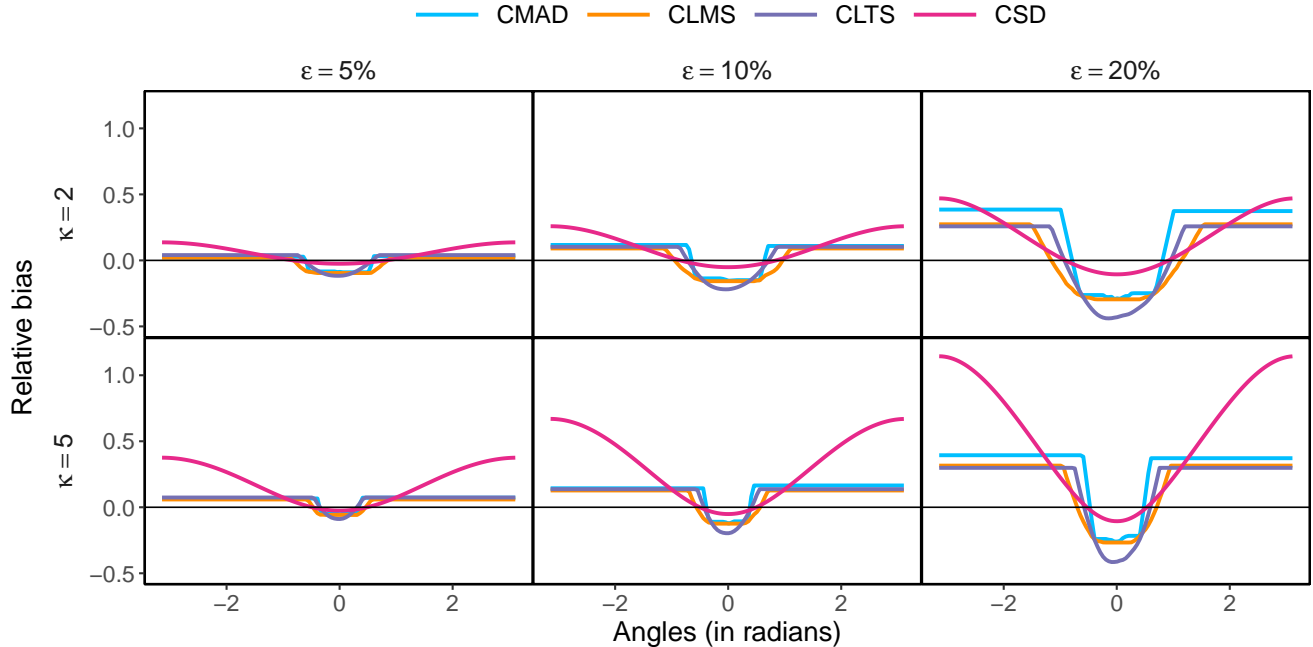


Figure 4: Relative bias curves of CMAD, CLMS, CLTS and CSD at von Mises distributions with  $\mu = 0$ . The rows are for concentration  $\kappa = 2, 5$ . The columns have contamination rate  $\varepsilon = 5\%, 10\%, 20\%$ .

The value of  $\kappa$  does not have a large impact on the size of the relative bias of the three robust measures. On the other hand, the CSD exhibits a much larger relative bias at higher  $\kappa$  values. This can be understood as follows. When  $\kappa$  is high, the uncontaminated data are tightly clustered around  $\mu$ , and the dispersion measure CSD is very precise with low variability. Then even a small amount of contamination can cause a noticeable relative change. In other words, when  $\kappa$  is high the CSD behaves like the classical standard deviation on the straight line.

These results are in line with those of [Ko and Guttorp \(1988\)](#). They consider a standardized version of the influence function, which is the influence function divided by  $S(F)$ . In (20) we standardize the bias in the same way. In their Theorem 4 they show that the standardized influence function of the classical dispersion estimator becomes unbounded as  $\kappa$  increases, and they conclude that this estimator is not robust.

Our results indicate that, from a relative bias point of view, the three proposed robust measures perform much better than CSD. Overall, CLMS has the smallest bias.

We performed a similar analysis under the mean shift outlier model, where the uncontaminated and contaminating distributions have equal values of  $\kappa$  and differ only in location. The results (not shown) are qualitatively similar to those in Figure 4.

## 6 Robust estimation of parameters of circular distributions

The proposed dispersion measures can be used to obtain robust estimators of parameters of circular distributions. We will illustrate this for von Mises distributions with concentration parameter  $\kappa$ , and for wrapped normal distributions with dispersion parameter  $\sigma$ .

We first look at the values of CMAD, CLMS, and CLTS as a function of the population CSD in Figure 5, that were obtained numerically. The dashed horizontal lines indicate their infimum and their supremum.

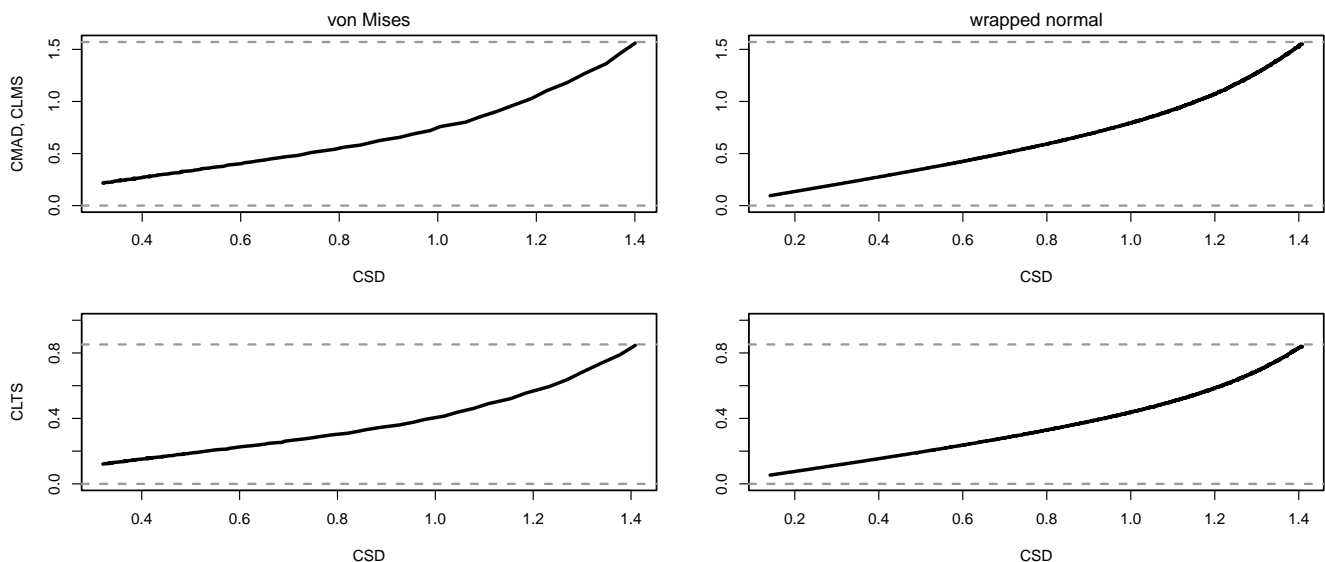


Figure 5: Values of the CMAD, CLMS, CLTS as a function of the population CSD at the von Mises distribution (left) with  $0 < \kappa \leq 10$ , and at the wrapped normal distribution with  $0 < \sigma \leq 3$ . Dashed lines correspond to the infimum and to the supremum of these circular measures.

Moreover, the population CSD is itself a nonlinear function of the concentration parameter  $\kappa$  of the von Mises distribution, and of the  $\sigma$  of the wrapped normal distribution, as seen in Figure 6 where the values of CSD are given as functions of  $\kappa$  for  $0 < \kappa \leq 10$ , and of  $\sigma$  for  $0 < \sigma \leq 3.4$ .

### 6.1 Robust consistent estimators of $\kappa$ and $\sigma$

We now use these relationships to construct robust and consistent estimators of the model parameters by first obtaining a robust estimate of the population CSD and then mapping it to the corresponding parameter  $\kappa$  or  $\sigma$  through an appropriate transformation.

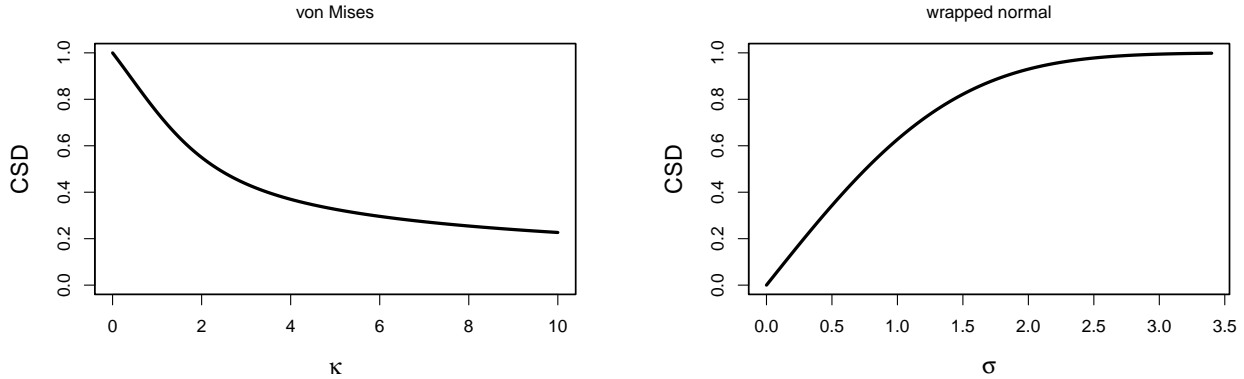


Figure 6: Values of CSD as a function of the parameters  $\kappa$  at the von Mises and  $\sigma$  at the wrapped normal.

Let  $S_n$  denote a robust circular dispersion measure computed from a sample  $\{\theta_1, \dots, \theta_n\}$ . For each circular model, the corresponding population dispersion measure  $S$  can be expressed as a function of the underlying CSD as

$$S = \eta(\text{CSD}).$$

By inverting this relationship we then obtain a robust estimator of the population CSD by

$$\widehat{\text{CSD}}_n = \eta^{-1}(S_n).$$

From this robust estimator of the population CSD we then derive consistent estimators of the corresponding parameters. For the von Mises distribution we obtain an estimator of  $\kappa$  by numerically inverting the function  $A(\kappa) = I_1(\kappa)/I_0(\kappa)$ , yielding the consistency function

$$\widehat{\kappa} = A^{-1}(\widehat{\rho}) = A^{-1}\left(1 - \frac{\widehat{\text{CSD}}_n^2}{2}\right).$$

For the wrapped normal we similarly construct the consistency function for the scale parameter  $\sigma$  as

$$\widehat{\sigma} = \sqrt{-2 \log(\widehat{\rho})} = \sqrt{-2 \log\left(1 - \frac{\widehat{\text{CSD}}_n^2}{2}\right)}.$$

In the linear setting the analogous consistency function is constant, so it becomes a consistency factor.

## 6.2 Breakdown values of CMAD, CLMS, and CLTS

A popular robustness measure of a functional is its breakdown value, defined as the highest fraction of outliers the functional can cope with. For a dispersion/concentration estimator, the implosion and explosion breakdown values are defined. The first is the smallest fraction of contamination

needed to drive the estimate down to zero, while the second is the smallest fraction of contamination needed to drive the estimate to its supremum.

A functional  $S$  is Fisher consistent for a parameter  $\psi$  of distributions  $F_\psi$  if always  $S(F_\psi) = \psi$ .

**Definition 6** (Breakdown values of a functional). The implosion and explosion breakdown values of a functional  $S$  at a circular distribution  $F$  are given by

$$\begin{aligned}\varepsilon_{\text{imp}}^*(S, F) &:= \inf\{\varepsilon > 0 : \inf_H S((1 - \varepsilon)F + \varepsilon H) = 0\} \\ \varepsilon_{\text{exp}}^*(S, F) &:= \inf\{\varepsilon > 0 : \sup_H S((1 - \varepsilon)F + \varepsilon H) = \sup S\}\end{aligned}$$

where  $H$  ranges over all circular distributions. The overall breakdown value is

$$\varepsilon^*(S, F) := \min\{\varepsilon_{\text{imp}}^*(S, F), \varepsilon_{\text{exp}}^*(S, F)\}.$$

Let  $\psi$  denote a circular dispersion parameter and let  $\hat{\psi}_S$  be an estimator defined by a strictly monotone consistency function of a robust dispersion measure  $S$  that is either CMAD, CLMS, or CLTS. Then the breakdown values of each  $\hat{\psi}_S$  are determined by those of the corresponding robust measure  $S$ , whose upper and lower bounds are given in Lemmas 2 to 5. These breakdown values are given below. The proofs are provided in Section C of the Supplementary Material.

**Lemma 6** (Upper bound for the implosion breakdown value of  $\hat{\psi}_{\text{CMAD}}$ ). *Let  $F$  be a unimodal and symmetric circular distribution with dispersion parameter  $\psi$ . We temporarily restrict the  $H$  in Definition 6 to those distributions for which  $G := (1 - \varepsilon)F + \varepsilon H$  has a unique circular median. Then*

$$\varepsilon_{\text{imp}}^*(\hat{\psi}_{\text{CMAD}}, F) < 1 - 0.5/[P_F(\mu - \pi/2 < \Theta < \mu + \pi/2)]. \quad (21)$$

*Therefore, for both the von Mises and the wrapped normal distributions, the implosion breakdown value of  $\hat{\psi}_{\text{CMAD}}$  is less than 0.5.*

**Theorem 8** (Overall breakdown value of  $\hat{\psi}_{\text{CMAD}}$ ). *Let  $F$  be a unimodal and symmetric circular distribution with dispersion or concentration parameter  $\psi > 0$ . We temporarily restrict the  $H$  in Definition 6 to those distributions for which  $G := (1 - \varepsilon)F + \varepsilon H$  has a unique circular median. Then*

$$\varepsilon_{\text{exp}}^*(\hat{\psi}_{\text{CMAD}}, F) = 0.5.$$

*Therefore the overall breakdown value of  $\hat{\psi}_{\text{CMAD}}$  satisfies the upper bound*

$$\varepsilon^*(\hat{\psi}_{\text{CMAD}}, F) < 1 - 0.5/[P_F(\mu - \pi/2 < \Theta < \mu + \pi/2)] < 0.5. \quad (22)$$

By Theorem 8, the breakdown value of  $\hat{\psi}_{\text{CMAD}}$  does not reach 0.5, the maximum attainable value. This contrasts with the MAD for linear data, whose breakdown value does reach 0.5.

On the other hand, although the breakdown value of CMAD does not attain the value 0.5, the upper bound can still be relatively high. Figure 7 shows the upper bound of the implosion breakdown value of CMAD at the von Mises model, as a function of the concentration parameter  $\kappa$ . For  $\kappa$  as low as two, we attain 0.459. The upper bound becomes close to 0.5 when the probability of the half circle  $P_F(\mu - \pi/2 < \Theta < \mu + \pi/2)$  approaches 1. Note that  $\hat{\kappa}_{\text{CMAD}}$  is a monotone decreasing function of CMAD, so it explodes when CMAD implodes, but its breakdown value remains the same as in Theorem 8.

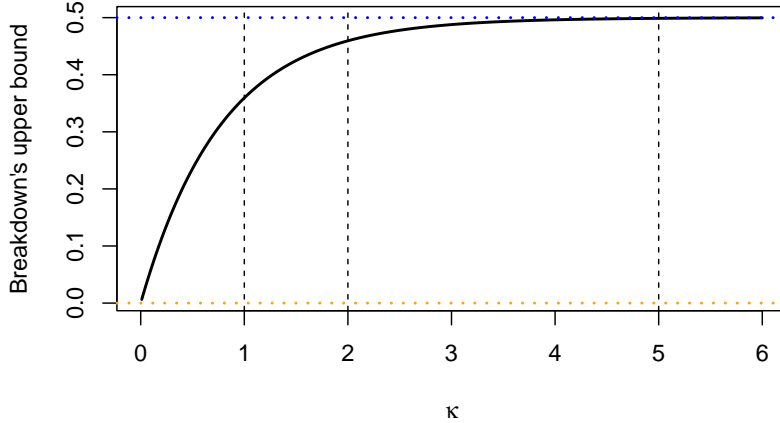


Figure 7: Upper bound for the breakdown value of  $\hat{\kappa}_{\text{CMAD}}$  as a function of the value of the concentration parameter  $\kappa$  under a von Mises distribution, from Theorem 8.

The estimator of  $\psi$  based on CLMS does attain the highest possible breakdown value.

**Theorem 9** (Breakdown value of  $\hat{\psi}_{\text{CLMS}}$ ). *Let  $F$  be a unimodal symmetric distribution with dispersion or concentration parameter  $\psi > 0$ , with estimator  $\hat{\psi}_{\text{CLMS}}$ . Then*

$$\varepsilon^*(\hat{\psi}_{\text{CLMS}}, F) = 0.5.$$

This follows directly from Lemmas 2 and 3.

**Theorem 10** (Breakdown value of  $\hat{\psi}_{\text{CLTS}}$ ). *Let  $F$  be a unimodal symmetric distribution with dispersion or concentration parameter  $\psi > 0$ , with estimator  $\hat{\psi}_{\text{CLTS}}$ . Then*

$$\varepsilon^*(\hat{\psi}_{\text{CLTS}}, F) = 0.5.$$

This result is analogous to Theorem 9. In particular, the implosion breakdown value is obtained from Lemma 4, and the explosion breakdown value from Lemma 5.

The breakdown properties of the estimators  $\hat{\psi}_{\text{CMAD}}$ ,  $\hat{\psi}_{\text{CLMS}}$  and  $\hat{\psi}_{\text{CLTS}}$  depend directly on the implosion and explosion breakdown values of the robust circular dispersion functionals CMAD, CLMS, and CLTS, and are therefore independent of the assumed parametric family.

### 6.3 Efficiencies of $\hat{\psi}_{\text{CMAD}}$ , $\hat{\psi}_{\text{CLMS}}$ , $\hat{\psi}_{\text{CLTS}}$

The efficiency of the proposed robust estimators is assessed through their asymptotic relative efficiency (ARE) with respect to the maximum likelihood estimator (MLE) under the assumed model. For a parameter of interest  $\psi$ , the ARE of an estimator  $\hat{\psi}$  is defined as

$$\text{ARE}(\hat{\psi}) = \text{AVar}(\hat{\psi}_{\text{MLE}}) / \text{AVar}(\hat{\psi})$$

where AVar stands for the asymptotic variance. These are derived in Section D of the Supplementary Material, and can be computed numerically.

For the von Mises distribution, the left panel of Figure 8 shows the ARE of the estimators  $\hat{\kappa}_{\text{CMAD}}$ ,  $\hat{\kappa}_{\text{CLMS}}$ , and  $\hat{\kappa}_{\text{CLTS}}$  over a grid of parameters  $\kappa$  ranging from 1 to 10. The ARE of  $\hat{\kappa}_{\text{CMAD}}$  and  $\hat{\kappa}_{\text{CLMS}}$  are the same, and are shown as the orange curve, while the ARE of  $\hat{\kappa}_{\text{CLTS}}$  is shown in purple.

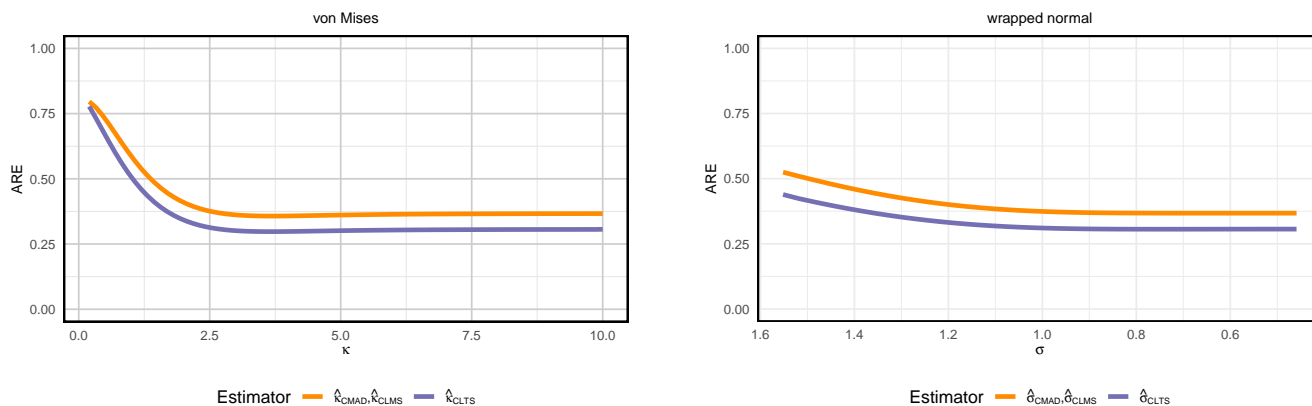


Figure 8: Asymptotic relative efficiency curves of the estimators based on CMAD, CLMS, and CLTS as a function of the concentration parameter  $\kappa$  at the von Mises and as a function of the dispersion parameter  $\sigma$  at the wrapped normal.

We see that the ARE decreases monotonically as  $\kappa$  increases. For low  $\kappa$ , the CMAD and CLMS based estimators retain over 70% efficiency relative to the MLE. As  $\kappa$  increases, the ARE goes down to around 37%. This horizontal asymptote was expected because when  $\kappa \rightarrow \infty$ , the von Mises distribution becomes locally similar to a normal distribution on the straight line, and the asymptotic efficiency of the linear MAD and LMS is indeed 36.74%.

The behavior of the CLTS based estimator of  $\kappa$  is similar for low  $\kappa$ . When  $\kappa$  increases the ARE lies a bit below that of  $\hat{\kappa}_{\text{CMAD}}$  and  $\hat{\kappa}_{\text{CLMS}}$ . In the limit for  $\kappa \rightarrow \infty$  it becomes 30.67% which is the efficiency of the LTS scale estimator at the normal distribution on the straight line, as derived in [Croux and Rousseeuw \(1992\)](#).

The right panel of Figure 8 shows the ARE of the estimators  $\hat{\sigma}_{\text{CMAD}}$ ,  $\hat{\sigma}_{\text{CLMS}}$ , and  $\hat{\sigma}_{\text{CLTS}}$  at the wrapped normal distribution. The parameter  $\sigma$  ranges from 0.45 to 1.55. Note that it is plotted from right to left on the horizontal axis to facilitate comparisons with the plot for the von Mises

distribution in the left panel, since a lower scale  $\sigma$  has a similar effect as a higher concentration  $\kappa$ . The orange curve is the ARE of  $\hat{\sigma}_{\text{CMAD}}$  and  $\hat{\sigma}_{\text{CLMS}}$ , and the purple curve is the ARE of  $\hat{\sigma}_{\text{CLTS}}$ . Again the CLTS-based estimator is a bit less efficient than the CLMS-based one, and for  $\hat{\sigma} \rightarrow 0$  we get the same limits as before, 36.74% for  $\hat{\sigma}_{\text{CLMS}}$  and 30.67% for  $\hat{\sigma}_{\text{CLTS}}$ .

Across both distributional models, we can conclude that the efficiency of the CLMS-based estimators slightly outperforms those based on CLTS.

## 6.4 Robustness of $\hat{\psi}_{\text{CMAD}}$ , $\hat{\psi}_{\text{CLMS}}$ , $\hat{\psi}_{\text{CLTS}}$ : an empirical study

So far we have studied the influence function, relative bias, and breakdown value. These are all based on functionals, that are population quantities. But of course we are also interested in the behavior on finite samples. For this purpose we performed a small simulation study about the impact of 10% and 20% of contamination.

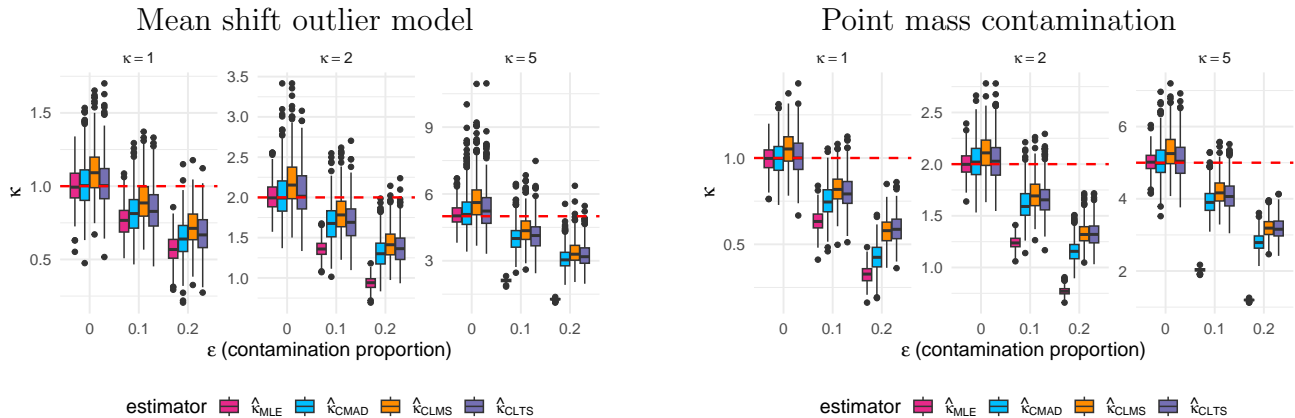


Figure 9: Simulation results for the von Mises distribution with  $\kappa \in \{1, 2, 5\}$ , with a fraction  $\varepsilon$  of antipodal contamination. The boxplots of the estimates  $\hat{\kappa}_{\text{MLE}}$ ,  $\hat{\kappa}_{\text{CMAD}}$ ,  $\hat{\kappa}_{\text{CLMS}}$ , and  $\hat{\kappa}_{\text{CLTS}}$  are shown together with the dashed red line at the true  $\kappa$ .

We start with the von Mises distribution, where we compare the effect of contamination on the maximum likelihood estimator  $\hat{\kappa}_{\text{MLE}}$  with that on  $\hat{\kappa}_{\text{CMAD}}$ ,  $\hat{\kappa}_{\text{CLMS}}$ , and  $\hat{\kappa}_{\text{CLTS}}$ . We generated 200 points from a von Mises distribution  $F$  with  $\mu(F) = 0$  and true concentration  $\kappa$  equal to 1, 2, and 5. Apart from this clean dataset, we also replaced 20 of its points (10%) by points from a von Mises distribution  $H$  with the same  $\kappa$  but with antipodal center, that is,  $\mu(H) = \pi$ . This mean shift outlier model is the worst contamination for location, see e.g. [Demni et al. \(2021\)](#). The same scenario was repeated for 20% of contamination. The experiments were replicated 500 times, with the results shown in the left panel of Figure 9. It contains a boxplot of  $\hat{\kappa}$  for each combination of  $\kappa$ ,  $\varepsilon$ , and estimator. For  $\varepsilon = 0$  (clean data) the medians of the four estimators are similar and

lie close to the dashed red horizontal line at the true  $\kappa$ , except for  $\hat{\kappa}_{\text{CLMS}}$  that has a small upward bias. The height of each box reflects the accuracy (efficiency) of the estimators. As expected, for clean data the MLE is the most accurate, but the other estimators still perform quite well. The situation changes for  $\varepsilon = 0.1$ , where the MLE is the most affected, followed by CMAD and then CLTS and CLMS. For  $\varepsilon = 0.2$  the effect is magnified, with the box of MLE far away and often small.

The right hand panel of Figure 9 is the result of a simulation with the same clean data, but now the 10% and 20% of contaminated data are all put in a single point, the antipodal point  $\pi$ . This is point mass contamination. We see that the effects are qualitatively similar to the left panel.

The simulation was repeated for the wrapped normal distribution, this time with the dispersion parameter  $\sigma$  taking the values 0.5, 1, and 1.2. The contamination was again of the mean shift outlier type, and point contamination. The results in Figure 10 look quite similar to those for the von Mises distribution, taking into account that the higher estimated dispersions  $\hat{\sigma}$  under contamination play the same role as the lower concentrations  $\hat{\kappa}$  before.

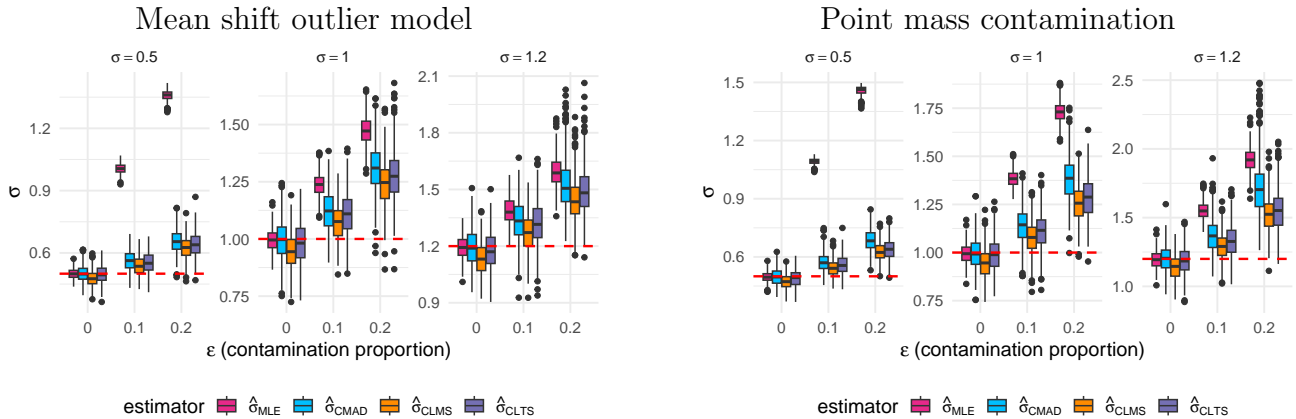


Figure 10: Simulation for the wrapped normal distribution with  $\sigma \in \{0.5, 1, 1.2\}$  and a fraction  $\varepsilon$  of antipodal contamination. The boxplots of  $\hat{\sigma}_{\text{MLE}}$ ,  $\hat{\sigma}_{\text{CMAD}}$ ,  $\hat{\sigma}_{\text{CLMS}}$ , and  $\hat{\sigma}_{\text{CLTS}}$  are shown together with the dashed red line at the true  $\sigma$ .

Overall, the simulation results indicate that the MLE estimator is the most affected by contamination, in both the von Mises and the wrapped normal models. The three robust estimators are much less affected. Between them, CLMS appears to be the most robust. Taken together with the results of the relative bias and the ARE, CLMS appears to be the best performing among the three robust methods.

## 7 Robust anomaly detection

In this section we will illustrate how robust estimation can be used for outlier detection on the circle.

### 7.1 A robust circular anomaly detection rule

There is a growing awareness of the effects of anomalous observations on data analysis, and the need for outlier detection methods for circular data. Some authors suggested techniques for circular outlier detection based on the deletion approach, see e.g. Collett (1980), Jammalamadaka and Sengupta (2001), and Mardia (1975). However, such procedures often suffer from the masking effect, meaning that an anomalous point cannot be detected in the presence of another outlier. Some of these techniques are only suitable for small sample sizes, or they assume that the concentration parameter is known beforehand.

Other approaches have also been proposed. However, some of them are only capable of detecting a single outlier (Abuzaid et al., 2012), while others use simulations under a specific data model to get cutoff values (Mahmood et al., 2017), or require that outliers be very well separated from the remainder of the data (Mohamed et al., 2016).

Also methodologies for outlier detection in toroidal and spherical data have been introduced by Abuzaid (2020), Greco et al. (2021), and Sau and Rodriguez (2018).

Some alternative methods based on robust measures have been developed. Both weighted likelihood and minimum disparity techniques have been adapted to the circular setting (Agostinelli, 2007). It turns out that the performance of these techniques depends strongly on the choice of certain parameters. In a related field, a robust outlier detection tool has been considered in circular regression (Rana et al., 2016).

Robust anomaly detection techniques assume that most of the data follow some parametric model. The parameters are then estimated robustly, and afterward the outliers are flagged by their large distance from the fitted model (Rousseeuw and Hubert, 2018).

Demni and Porzio (2023) applied this approach to circular data by assuming a von Mises distribution. However, the robust estimator of  $\kappa$  used was rather simple and presents high variability when the data are moderately concentrated.

In line with this approach, and making use of the results described above, we propose instead to use the CLMS-based estimator  $\hat{\kappa}_{\text{CLMS}}$  for the von Mises distribution, and the estimator  $\hat{\sigma}_{\text{CLMS}}$  for the wrapped normal. We also want the outlier detection rule to be invariant to rotation.

The proposed method first estimates the location robustly by the Fréchet median  $\tilde{\mu}$ , and then computes the shortest arc distances  $d(\theta_i, \tilde{\mu})$  of each circular observation  $\theta_i$  to  $\tilde{\mu}$ .

These distances are then compared with a cutoff value  $c_\alpha(\psi)$ , where  $\alpha > 0$  is the expected fraction of flagged points when the data are clean, and  $\psi$  is the dispersion or concentration parameter

of the underlying distribution. We estimate this parameter by the CLMS-based robust estimator such as  $\hat{\kappa}_{\text{CLMS}}$  or  $\hat{\sigma}_{\text{CLMS}}$ .

When the underlying circular distribution is symmetric about its location parameter, the cutoff value  $c_\alpha(\psi)$  is defined as the  $1 - \alpha/2$  quantile of the underlying distribution with center at  $\mu = 0$ . It thus corresponds to the numerical solution of the equation

$$\int_0^{c_\alpha(\psi)} f(\theta, \psi) d\theta = 1 - \alpha/2, \quad (23)$$

where  $f(\theta, \psi)$  is the density of the distribution with  $\mu = 0$ . Next, we flag a circular data point  $\theta_i$  whenever

$$d(\theta_i, \tilde{\mu}) > c_\alpha(\hat{\psi}_{\text{CLMS}}). \quad (24)$$

## 7.2 Visualizing anomalies: the circular violin plot

In addition to the outlier detection rule, we also provide a companion graphical tool, that we call a *circular violin plot*. Its goal is to enable further data analytic insights.

Violin plots on the straight line were introduced by [Hintze and Nelson \(1998\)](#). They were designed to overcome some limitations of traditional boxplots. When Tukey introduced boxplots little computing power was available, so their simplicity was an advantage, but that also limited the amount of information they could visualize. Violin plots contain a density estimate that can reveal multimodality. For an overview of linear violin plots and their uses see [Aberasturi \(2014\)](#). The violin plot has been widely adopted in various disciplines including biostatistics ([Mekkes et al., 2024](#)) and psychology ([Tanious and Manolov, 2022](#)). Several extensions of violin plots and related graphical tools have been proposed ([Montalcini and Rousseeuw, 2025](#)).

A violin plot for circular data has to respect the geometry of the circle. The estimated density is mounted on the circumference of the unit circle. This density curve is then mirrored radially on the inside of the circle. The area between the density curves forms a smooth ring whose thickness reflects the local data concentration. The density is estimated nonparametrically, using a von Mises kernel. The density is clipped at the cutoff threshold of the outlier detection rule, and data points lying outside the violin are flagged as outliers.

Inside the violin, elements of the circular boxplot ([Buttarazzi et al., 2018](#)) are integrated. The box represents the interquartile range with 25% of the data on either side of the median, highlighting the central 50% of the data. The median is indicated by a little white line. The median and the box visualize robust summaries of location and variability. We will illustrate the circular violin plot on real examples in the next section.

## 8 Real data analysis

Three real data examples are considered. The results shown are based on fitting the data by von Mises distributions, but using the wrapped normal distribution yields essentially the same results.

### 8.1 Northern cricket frogs data

Ferguson et al. (1967) collected data on the homing ability of Northern cricket frogs. After 30 hours in a dark environmental chamber, 14 frogs were released and their directions recorded. Results are reported in radians, with zero radians corresponding to East, and angles measured counterclockwise. The data are plotted in the left panel of Figure 11. Their circular sample median  $\hat{\mu} = 2.39$  radians is indicated by a black arrow. The CLMS-based robust estimate of the concentration parameter is  $\hat{\kappa}_{\text{CLMS}} = 3.88$ . From formula (23) we obtain the cutoff value  $c_{0.01}(\hat{\kappa}_{\text{CLMS}}) = 1.34$  radians.

The circular violin plot in the right panel is constructed by estimating the circular density using the robust estimate  $\hat{\kappa}_{\text{CLMS}}$ . The density is rescaled and displayed radially around the unit circle, yielding a symmetric violin shape. One observation is flagged as an outlier. This is in line with the literature: Collett (1980) found the same point (5.515 radians) to be a circular outlier, by means of a deletion approach.

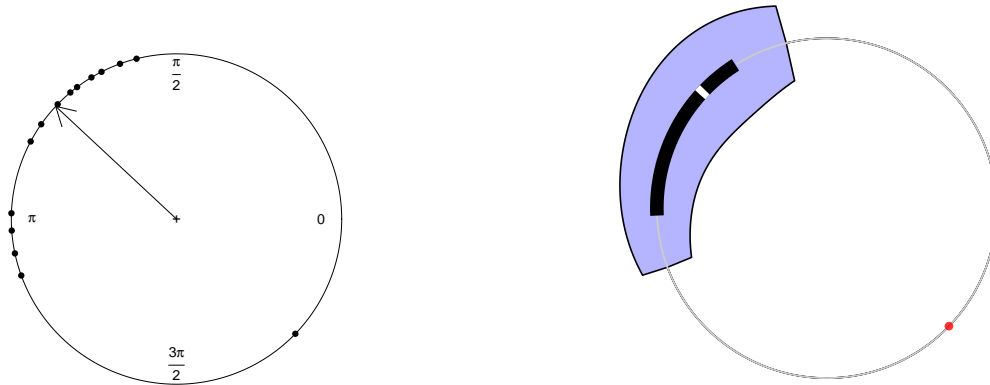


Figure 11: (Left) Plot of the Northern cricket frogs data with their sample circular median direction (black arrow), and (right) their circular violin plot.

At first sight one might think that the parts of the violin inside and outside the circle are not mirrored exactly, but they are. The perception is a consequence of the circular geometry itself, with its curvature and the closure of the circular domain. In a linear violin plot, the density is reflected across a straight axis, so equal distances on either side of the axis correspond to equal areas. On the circle, the mirroring is performed along radial directions, which does not translate into equal areas or visually symmetric shapes. As a result, one might perceive the mirrored density

as a single continuous band of varying thickness rather than as two symmetric halves. This effect is inherent in circular geometry and is independent of the specific density estimator or scaling choice.

## 8.2 Sardinian sea stars data

We saw the Sardinian sea stars data in Figure 1. They are the resultant directions of 22 sea stars, eleven days after being displaced from their natural habitat (Fisher, 1995). They are displayed in the left panel of Figure 12. The direction labeled as 0 radians (shown at the top) is the ‘correct’ direction of sea stars traveling toward the shore.

In this dataset, two points are far away from the majority of the data: one sea star (at 5.201 radians counterclockwise) moved along a longer route towards the shore, while the second (at 2.565 radians) navigated away from it. The question is whether these two points can be considered outliers.

If the single-value deletion technique in Collett (1980) is adopted, neither of them is flagged as outlying, due to the masking effect.

Kato and Eguchi (2016) also applied a single-value deletion technique. They compared robust estimates of the location and the concentration parameters of the von Mises distribution to the corresponding MLE estimates on subsamples where one point was omitted. They concluded that the point at 2.565 appears to be an outlier, while the outlyingness of the point at 5.201 was much more difficult to judge. This is understandable: if the furthest point is kept in the dataset, the omission of the second furthest does not have a large effect on the MLE.

A sequential deletion approach (i.e., deleting the most outlying observation and repeating the procedure) also has limitations in these data. According to the analysis in Fisher (1995), a von Mises Q-Q plot visually suggested that the point at 2.565 radians is discordant. But after deleting this point the von Mises Q-Q plot on the remaining data looked okay. The test for discordancy from the von Mises distribution did not reject the null hypothesis of no discordancy, so the point at 5.201 radians did not get flagged.

Our proposed outlier detection rule tells a different story. From the CLMS-based estimate  $\hat{\kappa}_{\text{CLMS}} = 7.92$  we obtain the threshold  $c_{0.01}(\hat{\kappa}_{\text{CLMS}}) = 0.86$  radians. The resulting circular violin plot is in the right panel of Figure 12. It clearly flags both far-out points as outliers. This is because  $\hat{\kappa}_{\text{CLMS}}$  uses only 50% of the data points to estimate  $\kappa$ , so neither of the two far-out points enter that calculation. On the other hand, if the MLE location  $\hat{\mu}_{\text{MLE}}$  and concentration  $\hat{\kappa}_{\text{MLE}}$  had been used in formula (24), the corresponding cutoff value would have been  $c_{0.01}(\hat{\kappa}_{\text{MLE}}) = 1.52$ , and then only the furthest point would have been flagged.

## 8.3 Drosophila fly larva data

Pewsey and Jones (2012) recorded changes in movement of a *Drosophila* fly larva, measured once

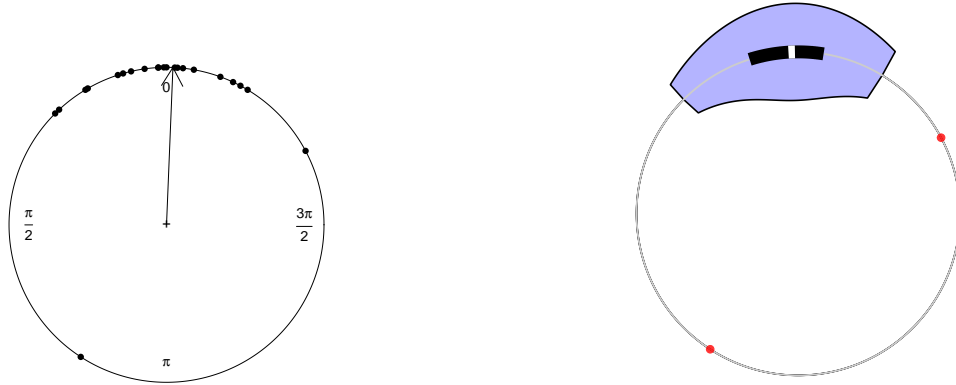


Figure 12: (Left) Plot of Sardinian sea stars data with circular median direction (black arrow), and (right) circular violin plot.

per second over a period of three minutes. The left panel of Figure 13 displays all 180 points, with the reference direction of 0 radians shown at the top. The sample circular median is  $\tilde{\mu} = 6.26$  radians (near the top) and the CLMS-based estimate of concentration is  $\hat{\kappa}_{\text{CLMS}} = 15.58$ . Assuming the data comes from a von Mises distribution, the corresponding cutoff value is  $c_{0.01}(\hat{\kappa}_{\text{CLMS}}) = 0.60$ .

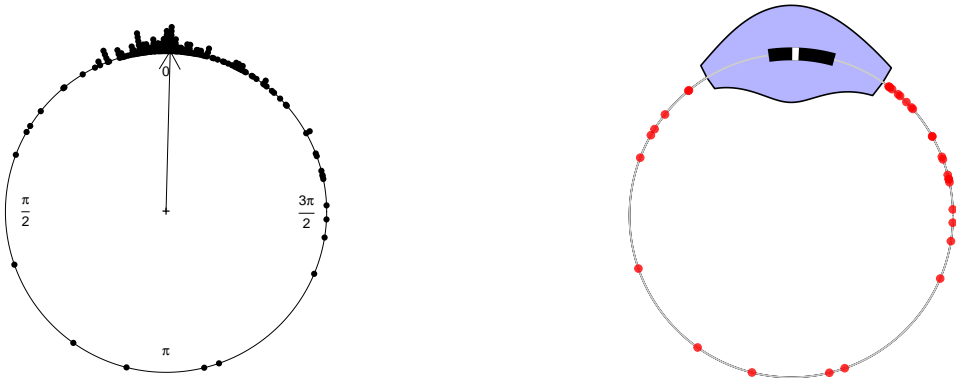


Figure 13: (Left) plot of the *Drosophila* fly larva data with its circular median (black arrow), and (right) its circular violin plot.

In the circular violin plot in the right panel, many points are flagged as outliers. Furthermore, there is no clear gap between the violin and the nearby ‘outliers’. This suggests that the data, rather than being generated by a von Mises distribution, come from a distribution with heavier tails. The results of [Pewsey and Jones \(2012\)](#) indeed suggest that the larva data can be better modeled by an Inverse Batschelet distribution. We conclude that the circular violin plot can be of some help in questioning the distributional model underlying the observed data.

## 9 Conclusions

When analyzing circular data it is important to be able to estimate its dispersion. Classical dispersion measures such as the circular standard deviation can be unduly affected by outliers. Here we investigated three robust estimators of dispersion, CMAD, CLMS, and CLTS, that are extensions of popular dispersion measures for linear data. Of these only CMAD was used before, but not yet analyzed by the tools of robust statistics. In this paper we did, by deriving the influence function, relative bias, breakdown value, and asymptotic efficiency of all three methods, and we performed a simulation study with clean and contaminated data. Comparing all of these results we concluded that CLMS performed the best.

We have also constructed an outlier detection rule based on CLMS, that is less vulnerable to masking than earlier approaches. It is accompanied by a new graphical display called a circular violin plot. These tools enabled us to analyze three real datasets with varying numbers of potential outliers.

While the present work focused on circular data, extensions to other manifolds such as the sphere or the torus would be of considerable interest.

**Software** A zip file with the R code and an example script reproducing the examples is available at [https://wis.kuleuven.be/statdatascience/code/circular\\_r\\_code.zip](https://wis.kuleuven.be/statdatascience/code/circular_r_code.zip).

**Funding** The research of H. Demni was supported by the Flanders Research Foundation (FWO) under a Grant for a scientific stay in Flanders V500325N, and was also carried out within the project ECS 0000024 “Ecosistema dell’innovazione - Rome Technopole” financed by EU in NextGenerationEU plan through MUR Decree n. 1051 23.06.2022 PNRR Missione 4 Componente 2 Investimento 1.5 - CUP H33C2200042000. The work of G. Porzio was funded by the project ECS 0000024 “Ecosistema dell’innovazione - Rome Technopole” financed by EU in NextGenerationEU plan through MUR Decree n. 1051 23.06.2022 PNRR Missione 4 Componente 2 Investimento 1.5 - CUP H33C2200042000.

## References

- D. T. Aberasturi. Violin plot. *Wiley StatsRef: Statistics Reference Online*, 1-7, 2014.
- A. H. Abuzaid. Identifying density-based local outliers in medical multivariate circular data. *Statistics in Medicine*, 39(21):2793–2798, 2020.
- A. H. Abuzaid, A. G. Hussin, A. Rambli, and I. Mohamed. Statistics for a new test of discordance

- in circular data. *Communications in Statistics: Simulation and Computation*, 41(10):1882–1890, 2012.
- C. Agostinelli. Robust estimation for circular data. *Computational Statistics and Data Analysis*, 51(12):5867–5875, 2007.
- D. Buttarazzi, G. Pandolfo, and G. C. Porzio. A boxplot for circular data. *Biometrics*, 74(4):1492–1501, 2018.
- D. Collett. Outliers in circular data. *Journal of the Royal Statistical Society: Series C (Applied Statistics)*, 29(1):50–57, 1980.
- C. Croux and G. Haesbroeck. Maxbias curves of robust scale estimators based on subranges. *Metrika*, 53:101–122, 2001.
- C. Croux and P. J. Rousseeuw. A class of high-breakdown scale estimators based on subranges. *Communications in Statistics – Theory and Methods*, 21:1935–1951, 1992.
- H. Demni, A. Messaoud, and G. C. Porzio. Distance-based directional depth classifiers: a robustness study. *Communications in Statistics: Simulation and Computation*, 52(11):5695–5713, 2021.
- H. Demni and G. C. Porzio. Anomaly detection in circular data. In *SEAS 2023 Book of Short Papers*, pages 63–68, 2023.
- M. Di Marzio, S. Fensore, A. Panzera, and C. C. Taylor. Density estimation for circular data observed with errors. *Biometrics*, 78(1):248–260, 2022.
- D. E. Ferguson, H. F. Landreth, and J. P. Mckeown. Sun compass orientation of the northern cricket frog, *Acris crepitans*. *Animal Behaviour*, 15(1):45–53, 1967.
- J. J. Fernández-Durán. Models for circular–linear and circular–circular data constructed from circular distributions based on nonnegative trigonometric sums. *Biometrics*, 63(2):579–585, 2007.
- N. I. Fisher. *Statistical Analysis of Circular Data*. Cambridge University Press, 1995.
- L. Greco, G. Saraceno, and C. Agostinelli. Robust fitting of a wrapped normal model to multivariate circular data and outlier detection. *Stats*, 4(2):454–471, 2021.
- F. R. Hampel, E. M. Ronchetti, P. Rousseeuw, and W. A. Stahel. *Robust Statistics: The Approach Based on Influence Functions*. Wiley Interscience, New York, 1986.
- F. Hassanzadeh. A smoothing spline model for multimodal and skewed circular responses: Applications in meteorology and oceanography. *Environmetrics*, 32(2):e2655, 2021.

- J. L. Hintze and R. D. Nelson. Violin plots: a box plot-density trace synergism. *The American Statistician*, 52(2):181–184, 1998.
- S. R. Jammalamadaka and A. Sengupta. *Topics in Circular Statistics*. World Scientific, 2001.
- M. C. Jones and A. Pewsey. Inverse Batschelet distributions for circular data. *Biometrics*, 68(1):183–193, 2012.
- S. Kato and S. Eguchi. Robust estimation of location and concentration parameters for the von Mises–Fisher distribution. *Statistical Papers*, 57:205–234, 2016.
- D. Ko and P. Guttorp. Robustness of estimators for directional data. *The Annals of Statistics*, 16:609–618, 1988.
- C. Ley, and T. Verdebout. *Modern Directional Statistics*. Chapman and Hall/CRC, 2017.
- C. Ley, and T. Verdebout. *Applied Directional Statistics. Modern Methods and Case Studies*. CRC Press, Taylor and Francis, 2019.
- C. Leys, C. Ley, O. Klein, P. Bernard, and L. Licata. Detecting outliers: do not use standard deviation around the mean, use absolute deviation around the median. *Journal of Experimental Social Psychology*, 49:764–766, 2013.
- U. Lund and C. Agostinelli. Circular. R package version 0.5-0. <https://cran.r-project.org/web/packages/circular/circular.pdf>, 2013.
- E. A. Mahmood, S. Rana, H. Midi, and A. G. Hussin. Detection of outliers in univariate circular data using robust circular distance. *Journal of Modern Applied Statistical Methods*, 16:418–438, 2017.
- K. V. Mardia. *Statistics of Directional Data*. Academic Press, London, 1972.
- K. V. Mardia. Statistics of directional data. *Journal of the Royal Statistical Society Series B: Statistical Methodology*, 37(3):349–371, 1975.
- K. V. Mardia, C. C. Taylor, and G. K. Subramaniam. Protein bioinformatics and mixtures of bivariate von Mises distributions for angular data. *Biometrics*, 63(2):505–512, 2007.
- R. D. Martin and R. H. Zamar. Asymptotically min—max bias robust M-estimates of scale for positive random variables. *Journal of the American Statistical Association*, 84(406):494–501, 1989.

- N. J. Mekkes, M. Groot, E. Hoekstra, A. de Boer, E. Dagkesamanskaia, S. Bouwman, ..., I. R. Holtman. Identification of clinical disease trajectories in neurodegenerative disorders with natural language processing. *Nature Medicine*, 30(4):1143–1153, 2024.
- I. B. Mohamed, A. Rambli, N. Khaliddin, and A. I. N. Ibrahim. A new discordancy test in circular data using spacings theory. *Communications in Statistics: Simulation and Computation*, 45(8):2904–2916, 2016.
- C. M. Montalcini and P. J. Rousseeuw. The bixplot: A variation on the boxplot suited for bimodal data. *arXiv*, 2510.09276, 2025.
- S. Nagy, H. Demni, D. Buttarazzi, and G. C. Porzio. Theory of angular depth for classification of directional data. *Advances in Data Analysis and Classification*, 18(3):627–662, 2024.
- B. S. Otieno and C. M. Anderson-Cook. Measures of preferred direction for environmental and ecological circular data. *Environmental and Ecological Statistics*, 13:311–324, 2006.
- S. Rana, E. A. Mahmood, H. Midi, and A. G. Hussin. Robust detection of outliers in both response and explanatory variables of the simple circular regression model. *Malaysian Journal of Mathematical Sciences*, 10(3):399–414, 2016.
- M. Ranalli and A. Maruotti. Model-based clustering for noisy longitudinal circular data, with application to animal movement. *Environmetrics*, 31(2):e2572, 2020.
- P. J. Rousseeuw. Least median of squares regression. *Journal of the American Statistical Association*, 79:871–880, 1984.
- P. J. Rousseeuw and A. M. Leroy. *Robust Regression and Outlier Detection*. John Wiley & Sons, 1987.
- P. J. Rousseeuw and M. Hubert. Anomaly detection by robust statistics. *Wiley Interdisciplinary Reviews: Data Mining and Knowledge Discovery*, 8(2):e1236, 2018.
- W. D. Schutte and J. W. H. Swanepoel. SOPIE: an R package for the non-parametric estimation of the off-pulse interval of a pulsar light curve. *Monthly Notices of the Royal Astronomical Society*, 461(1):627–640, 2016.
- S. Seader, P. Tenenbaum, J. M. Jenkins, and C. J. Burke.  $\chi^2$  discriminators for transiting planet detection in Kepler data. *The Astrophysical Journal Supplement Series*, 206(2):25, 2013.
- M. F. Sau and D. Rodriguez. Minimum distance method for directional data and outlier detection. *Advances in Data Analysis and Classification*, 12:587–603, 2018.

R. Tanius and R. Manolov. Violin plots as visual tools in the meta-analysis of single-case experimental designs. *Methodology*, 18(3):221–238, 2022.

S. V. Tishkovskaya and P. G. Blackwell. Bayesian estimation of heterogeneous environments from animal movement data. *Environmetrics*, 32(6):e2679, 2021.

# Supplementary Material

## A: Robust dispersion measures

### Proof of Lemma 1

To prove Lemma 1, we first state an intermediate Lemma.

**Lemma 7.** *Let  $\Theta$  be a circular random variable, and  $\theta^* \in [-\pi, \pi)$  be such that  $P(\Theta = \theta^*) \geq 0.5$ , then the circular median set  $M_\theta = \{\theta^*\}$ . That is,  $\theta^*$  is the circular median of  $\Theta$ .*

*Proof.* Consider a value  $\delta \in [-\pi, \pi)$  such that  $\delta > \theta^*$ . We prove that

$$\mathbb{E}(d(\Theta, \delta)) \geq \mathbb{E}(d(\Theta, \theta^*)) \quad \forall \delta > \theta^*. \quad (25)$$

Since the case  $\delta < \theta^*$  follows by symmetry, this implies  $M_\theta = \theta^*$ , by definition of the circular median.

Let  $\gamma \in [-\pi, \pi)$ . By the properties of arc distances, we have that

$$d(\gamma, \delta) - d(\gamma, \theta^*) = \begin{cases} d(\delta, \theta^*) & \text{if } \gamma \leq \theta^* \\ > -d(\delta, \theta^*) & \text{if } \gamma > \theta^* \end{cases} \quad \forall \delta > \theta^*.$$

Hence, by considering the difference  $\mathbb{E}(d(\Theta, \delta)) - \mathbb{E}(d(\Theta, \theta^*))$  and conditioning, we have  $\mathbb{E}(d(\Theta, \delta) - d(\Theta, \theta^*)) \geq d(\delta, \theta^*)P(\Theta \leq \theta^*) - d(\delta, \theta^*)P(\Theta > \theta^*) = d(\delta, \theta^*)(P(\Theta \leq \theta^*) - P(\Theta > \theta^*)) \geq 0$ , since  $P(\Theta = \theta^*) \geq 0.5$  by assumption.  $\square$

Note that, by the same argument, if  $P(\Theta = \theta^*) > 0.5$ , then  $\mathbb{E}(d(\Theta, \delta)) > \mathbb{E}(d(\Theta, \theta^*)) \forall \delta > \theta^*$ , and  $\theta^*$  is the unique minimizer. Hence,  $\Theta \in \mathcal{M}_1$ .

The proof of Lemma 1 follows, equation by equation.

*Proof.* If  $\exists \theta : P(\Theta = \theta) > 0.5$ , then  $M_\theta = \theta$  and  $\Theta \in \mathcal{M}_1$  according to the above lemma. We thus have  $P(d(\Theta, \theta) = 0) > 0.5$ , and  $P(d(\Theta, \theta) \geq 0) > 0.5$ . Hence, by definition of the linear median,  $\text{CMAD}(F) = 0$ .

If  $\exists \theta : P(\Theta = \theta) = 0.5$ , then  $\theta$  belongs to the set  $M_\theta$  according to the above lemma. If that set contains more than one element, then the CMAD is undefined. If it is a singleton instead, then the distribution of the distances  $d(\Theta, \theta)$  can have median equal to zero, or zero can be the extreme of a (linear) median set. In the first case (for instance when  $F = 0.5\Delta_\theta + 0.5G$ , with  $\Delta_\theta$  a point mass distribution located in  $\theta$  and  $G \sim \text{Uniform}(-\pi, \pi)$ ),  $\text{CMAD}(F) = 0$ . In the second case (e.g., if  $F = 0.2\Delta_{\theta-\pi/8} + 0.5\Delta_\theta + 0.3\Delta_{\theta+\pi/6}$ ),  $\text{CMAD}(F) > 0$  being CMAD the midpoint of an interval

of positive length that has an extreme in zero (this happens because the cdf of the distribution of the distances from  $\theta$  is a function that takes value 0.5 from zero up to a certain point). Finally, because the distance distribution is bounded by  $\pi$ , we also have  $\text{CMAD}(F) < \pi/2$ . The equality cannot be reached because it would necessarily require that  $F = 0.5\Delta_\theta + 0.5\Delta_{\theta \pm \pi}$ , which is indeed a case of  $\Theta \notin \mathcal{M}_1$ .

If  $\forall \theta P(\Theta = \theta) < 0.5$ , then the distribution of the distances from  $\theta$  cannot have median equal to zero and therefore  $\text{CMAD}(F) > 0$ . Furthermore, that median cannot reach the value of  $\pi$ . Because the circle is bounded, the distribution of the shortest arc distance has its maximum achievable value equal to  $\pi$ , and hence  $\text{CMAD}(F) \leq \pi$ . However, to get  $\text{CMAD} = \pi$ , the (linear) median should be equal to the maximum achievable value of the distance distribution. This can occur only if at least half of the probability is in the upper tail of the distance distribution, which in turn implies that (at least) half of the probability is pointwise located somewhere on the circle. However, by the above Lemma,  $\text{CMAD}$  would be either equal to 0, or to a set that includes 0, not to  $\pi$ . Consequently,  $\text{CMAD}(F) < \pi, \forall \Theta \in \mathcal{M}_1$ .  $\square$

**Proof of Theorem 1** To prove the theorem, we show there exists a family of distributions for the supremum of  $\text{CMAD}$  is  $\pi$ . To start, consider the distributions

$$F = \lambda\Delta_0 + 0.5(1 - \lambda)\Delta_{c\pi} + 0.5(1 - \lambda)\Delta_{-c\pi}, \quad 0 \leq \lambda < 0.5, \quad 0 < c < 1.$$

for  $c > 0$ . Note that we set  $\lambda < 0.5$  because if  $\lambda \geq 0.5$  we would have  $0 \leq \text{CMAD}(F) < \pi/2$  by Lemma 1. The case  $c = 0$  is not interesting (we obtain a point mass in 0, and  $\text{CMAD}(F)$  will be equal to zero again). For  $c = 1$ ,  $F$  becomes  $\lambda\Delta_0 + (1 - \lambda)\Delta_\pi$  and again  $\text{CMAD}(F) = 0$  for  $\lambda < 0.5$  by Lemma 1.

At these distributions we derive the expected value  $\mathbb{E}(d(\theta, \phi))$  as a function of the generic angle  $\theta$ . For the sake of simplicity, and without loss of generality by the symmetry of the distribution around 0, we investigate it only for  $0 \leq \theta \leq \pi$ . We have:

$$\begin{aligned} \mathbb{E}(d(\Theta, \theta)) &= (1 - \lambda)d(\theta, 0) + 0.5\lambda d(\theta, c\pi) + 0.5\lambda d(\theta, -c\pi) \\ &= (1 - \lambda)\theta + 0.5\lambda(d(\theta, c\pi) + d(\theta, -c\pi)). \end{aligned}$$

We will distinguish three cases. First, suppose  $0 \leq \theta \leq -c\pi + \pi$ . If so, we will have that  $d(\theta, c\pi) + d(\theta, -c\pi) = 2c\pi$ . If instead  $-c\pi + \pi \leq \theta \leq c\pi$ , then  $d(\theta, c\pi) + d(\theta, -c\pi) = 2((c\pi - \theta) + (\pi - c\pi)) = 2(\pi - \theta)$ . Finally, if  $c\pi \leq \theta \leq \pi$ , then  $d(\theta, c\pi) + d(\theta, -c\pi) = 2(1 - c)\pi$ . In brief, for  $0 \leq \theta \leq \pi$  we can write:

$$\mathbb{E}(d(\Theta, \theta)) = \lambda\theta + (1 - \lambda) * \begin{cases} c\pi & 0 \leq \theta \leq (1 - c)\pi \\ \pi - \theta & (1 - c)\pi < \theta \leq c\pi \\ (1 - c)\pi & c\pi < \theta \leq \pi. \end{cases} \quad (26)$$

This is a piecewise linear function that increases from 0 to  $(1 - c)\pi$ , decreases from  $(1 - c)\pi$  up to  $c\pi$ , and increases again from  $c\pi$  to  $\pi$ . As a consequence, extending the result to the whole circle, the median set  $M_\theta$  can only be  $\{0\}$  or  $\{c\pi, -c\pi\}$ . In the latter case, CMAD is not defined.

We are interested in the first case. By definition of circular median, it occurs if  $\mathbb{E}(d(\Theta, 0)) < \mathbb{E}(d(\Theta, c\pi))$ . That is, by Equation (26), if

$$(1 - \lambda)c\pi < \lambda c\pi + (1 - \lambda)(1 - c)\pi. \quad (27)$$

This condition is satisfied whenever  $c < (1 - \lambda)/(2 - 3\lambda)$ . Hence, the circular random variable  $\Theta'$  with

$$F' := \lambda\Delta_0 + 0.5(1 - \lambda)\Delta_{c\pi} + 0.5(1 - \lambda)\Delta_{-c\pi}, \quad 0 \leq \lambda < 0.5, \quad 0 < c < (1 - \lambda)/(2 - 3\lambda), \quad (28)$$

has  $M_{\theta'} = \{0\}$  by construction. Furthermore, it holds that  $\text{CMAD}(F') = c\pi$ . This is because the distance distribution from  $M_{\theta'}$  is a linear combination of two point mass distributions, one in 0 (with probability  $\lambda < 0.5$ ), and one in  $c\pi$ . As a consequence, given that  $\lim_{\lambda \rightarrow 0.5} (1 - \lambda)/(2 - 3\lambda) = 1$ ,

$$\sup_{\lambda, c} \text{CMAD}(F') = \sup_{\lambda, c} c\pi = \pi.$$

### Proof of Theorem 3

( $\Rightarrow$ ) If  $\Theta \sim H_{0.5}$ , then the length of each arc with probability mass at least 0.5 is exactly equal to  $\pi$ . The result follows from Equation (8).

( $\Leftarrow$ ) Suppose that  $\Theta$  has distribution  $H \neq H_{0.5}$ . By definition, it implies there exists at least one semicircle  $HC^*$  such that  $\int_{HC^*} dH(\theta) \neq 0.5$ . If so, either  $\int_{HC^*} dH(\theta) > 0.5$  and  $\int_{\overline{HC^*}} dH(\theta) < 0.5$  or  $\int_{HC^*} dH(\theta) < 0.5$  and  $\int_{\overline{HC^*}} dH(\theta) > 0.5$  (here,  $\overline{HC^*}$  is the complement to  $\mathcal{S}$  of  $HC^*$ ). In both cases, there will be at least an arc  $A$  of length  $\ell(A) = a < \pi$  such that  $\int_A dH(\theta) = 0.5$ . Hence, by Equation (8), we would have  $\text{CLMS}(H) = a/2 < \pi/2$ , which contradicts the hypothesis.

## B: Influence functions

### Proof of Theorem 6

We start with CMAD. The population circular median of the uncontaminated distribution  $F$  is unique due to the fact that  $F$  is strictly unimodal, and equals the center of symmetry 0. The median arc length from the population median is thus equal to

$$\text{CMAD}(F) = F^{-1}\left(\frac{3}{4}\right) - F^{-1}\left(\frac{1}{2}\right) = F^{-1}\left(\frac{3}{4}\right).$$

We will denote  $q := F^{-1}(3/4)$  for brevity.

Now let us contaminate  $F$ , yielding  $F_\varepsilon := (1 - \varepsilon)F + \varepsilon\Delta_\theta$ . The cumulative distribution function  $F_\varepsilon$  is continuous on  $[-\pi, \theta[$ , where  $F_\varepsilon$  has the expression  $F_\varepsilon(u) = (1 - \varepsilon)F(u)$ . We will denote the circular median of the contaminated distribution  $F_\varepsilon$  as  $t(\varepsilon) := T(F_\varepsilon)$ . The uncontaminated distribution has  $\varepsilon = 0$ , so  $t(0) = 0$  as indicated in Figure S1. We also denote the CMAD of  $F_\varepsilon$  by  $s(\varepsilon)$ , with  $s(0)$  being the CMAD of the uncontaminated distribution  $F$ . For  $\varepsilon > 0$  the figure changes, as both  $t(\varepsilon)$  and  $s(\varepsilon)$  can move. The endpoints of the CMAD interval now become  $t(\varepsilon) - s(\varepsilon)$  and  $t(\varepsilon) + s(\varepsilon)$ .

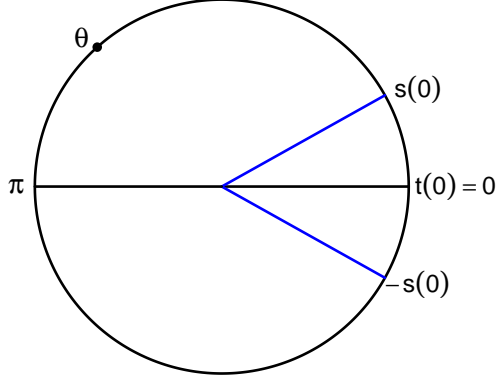


Figure S1: Sketch of the first part of the proof for CMAD, where  $q < \theta < \pi$ .

We first consider the situation where the contaminating point  $-\pi < \theta < \pi$  lies outside the original interval, that is,  $|\theta| > s(0)$ . Due to symmetry of  $F$  we can assume without loss of generality that  $\theta > s(0)$ , as in Figure S1. Note that for  $\varepsilon$  small enough we still have  $\theta > t(\varepsilon) + s(\varepsilon)$  because  $\theta > q = \lim_{\varepsilon \downarrow 0} s(\varepsilon) = \lim_{\varepsilon \downarrow 0} (t(\varepsilon) + s(\varepsilon))$ .

By the definition of CMAD the mass of  $F_\varepsilon$  between the endpoints must be one half, so

$$\begin{aligned} F_\varepsilon(t(\varepsilon) + s(\varepsilon)) - F_\varepsilon(t(\varepsilon) - s(\varepsilon)) &= \frac{1}{2} \\ (1 - \varepsilon)F(t(\varepsilon) + s(\varepsilon)) - (1 - \varepsilon)F(t(\varepsilon) - s(\varepsilon)) &= \frac{1}{2}. \end{aligned}$$

Differentiating both sides of this equation with respect to  $\varepsilon$  yields

$$\begin{aligned} -1 \left( F(s(0)) - F(-s(0)) \right) + f(s(0)) \left( \frac{\partial t(\varepsilon)}{\partial \varepsilon} + \frac{\partial s(\varepsilon)}{\partial \varepsilon} \right) \\ - f(-s(0)) \left( \frac{\partial t(\varepsilon)}{\partial \varepsilon} - \frac{\partial s(\varepsilon)}{\partial \varepsilon} \right) &= 0 \\ -\frac{1}{2} + f(s(0)) \left( 2 \frac{\partial s(\varepsilon)}{\partial \varepsilon} \right) &= 0 \\ \text{IF}(\theta; \text{CMAD}, F) = \frac{\partial s(\varepsilon)}{\partial \varepsilon} &= \frac{1}{4f(F^{-1}(\frac{3}{4}))} \end{aligned}$$

in which  $\frac{\partial t(\varepsilon)}{\partial \varepsilon}$  has canceled.

We now consider the case where  $|\theta| < q$ . Figure S2 illustrates this for  $\theta > 0$ , but the situation  $\theta \leq 0$  is analogous. For  $\varepsilon$  small enough we have  $\theta < t(\varepsilon) + s(\varepsilon)$  because  $y < s(0) = \lim_{\varepsilon \downarrow 0} (t(\varepsilon) + s(\varepsilon))$ .

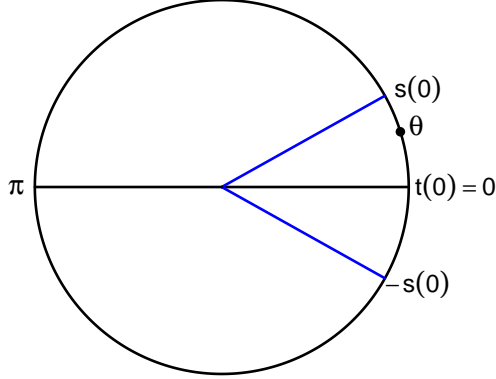


Figure S2: Sketch of the second part of the proof for CMAD, where  $-q < \theta < q$ .

By the definition of CMAD the mass of  $F_\varepsilon$  between the endpoints is again one half, but since  $t(\varepsilon) + s(\varepsilon) > \theta$  the expression of  $F_\varepsilon$  has an additional term  $\varepsilon$ , yielding

$$\begin{aligned} F_\varepsilon(t(\varepsilon) + s(\varepsilon)) - F_\varepsilon(t(\varepsilon) - s(\varepsilon)) &= \frac{1}{2} \\ (1 - \varepsilon)F(t(\varepsilon) + s(\varepsilon)) + \varepsilon - (1 - \varepsilon)F(t(\varepsilon) - s(\varepsilon)) &= \frac{1}{2}. \end{aligned}$$

Differentiating both sides of this equation with respect to  $\varepsilon$  yields

$$\begin{aligned} -1 \left( F(s(0)) - F(-s(0)) \right) + 1 + f(s(0)) \left( \frac{\partial t(\varepsilon)}{\partial \varepsilon} + \frac{\partial s(\varepsilon)}{\partial \varepsilon} \right) \\ - f(-s(0)) \left( \frac{\partial t(\varepsilon)}{\partial \varepsilon} - \frac{\partial s(\varepsilon)}{\partial \varepsilon} \right) &= 0 \\ -\frac{1}{2} + 1 + f(s(0)) \left( 2 \frac{\partial s(\varepsilon)}{\partial \varepsilon} \right) &= 0 \\ \text{IF}(\theta; \text{CMAD}, F) = \frac{\partial s(\varepsilon)}{\partial \varepsilon} &= \frac{-1}{4f(F^{-1}(\frac{3}{4}))}. \end{aligned}$$

Combining the expressions for  $|\theta| > q$  and  $|\theta| < q$  yields the formula in the theorem.

We now turn to the circular Least Median Spread. Due to the assumptions on  $F$ , the mini-

mization of (16) can be carried out by setting the first derivative of the objective to zero:

$$\begin{aligned} \frac{\partial}{\partial t} \frac{1}{2} \left( F^{-1} \left( t + \frac{1}{2} \right) - F^{-1}(t) \right) &= 0 \\ \frac{1}{f \left( F^{-1} \left( t + \frac{1}{2} \right) \right)} - \frac{1}{f \left( F^{-1}(t) \right)} &= 0 \\ F^{-1} \left( t + \frac{1}{2} \right) &= F^{-1}(1 - t) \\ t + \frac{1}{2} &= 1 - t \\ t &= \frac{1}{4} \end{aligned}$$

hence

$$\text{CLMS}(F) = \frac{1}{2} \left( F^{-1} \left( \frac{3}{4} \right) - F^{-1} \left( \frac{1}{4} \right) \right) = F^{-1} \left( \frac{3}{4} \right).$$

We again denote  $q := F^{-1}(3/4)$ .

We now switch to the contaminated distribution  $F_\varepsilon := (1 - \varepsilon)F + \varepsilon\Delta_\theta$ . We first consider the situation where  $q < |\theta| \leq \pi$ . We assume w.l.o.g. that  $\theta > q$ , the case  $\theta < -q$  being analogous by symmetry. The situation is sketched in Figure S3. The distribution function  $F_\varepsilon$  is continuous on  $[-\pi, \theta[$  where  $F_\varepsilon$  has the expression  $F_\varepsilon(u) = (1 - \varepsilon)F(u)$ . Therefore the total mass strictly to the left of  $\theta$  is  $P_\varepsilon[-\pi < u < \theta] = (1 - \varepsilon)F(\theta)$ . For any  $\varepsilon < (F(\theta) - F(q))/F(\theta)$  it then holds that  $(1 - \varepsilon)F(\theta) > F(\theta) - F(\theta) + F(q) = F(q) = \frac{3}{4}$ . Therefore the total mass of  $F_\varepsilon$  strictly to the left of  $\theta$  is over  $\frac{3}{4}$ . This is where we will look for the shortest half.

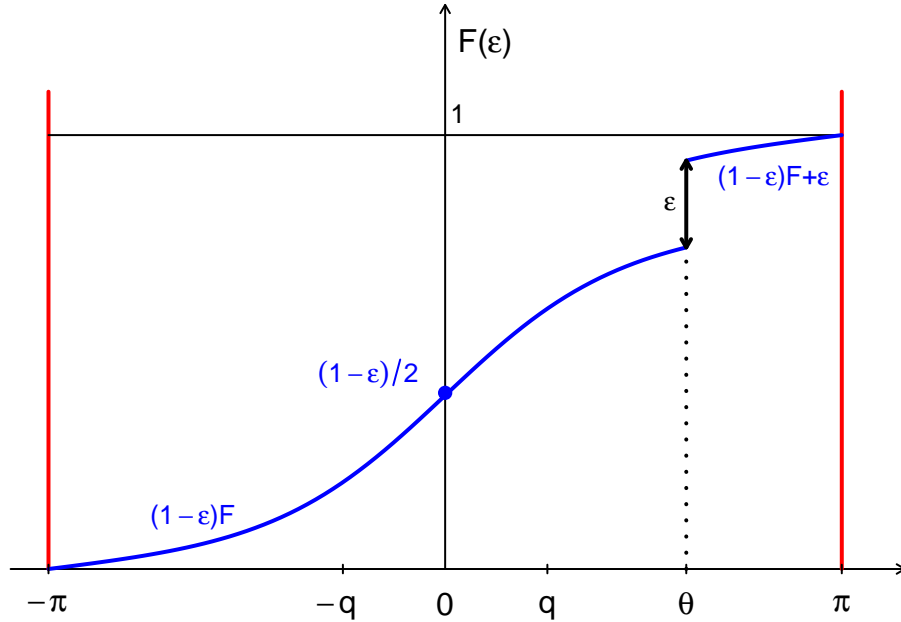


Figure S3: Sketch of the first part of the proof for CLMS, where  $q < \theta \leq \pi$ .

Minimizing (16) over this region where  $F_\varepsilon$  is smooth, we find

$$\begin{aligned}
\frac{\partial}{\partial t} \frac{1}{2} \left( F_\varepsilon^{-1} \left( t + \frac{1}{2} \right) - F_\varepsilon^{-1} (t) \right) &= 0 \\
\frac{\partial}{\partial t} \left( F^{-1} \left( \left( t + \frac{1}{2} \right) / (1 - \varepsilon) \right) - F^{-1} \left( t / (1 - \varepsilon) \right) \right) &= 0 \\
f \left( F^{-1} \left( \left( t + \frac{1}{2} \right) / (1 - \varepsilon) \right) \right) &= f \left( F^{-1} \left( t / (1 - \varepsilon) \right) \right) \\
F^{-1} \left( \left( t + \frac{1}{2} \right) / (1 - \varepsilon) \right) &= F^{-1} \left( 1 - t / (1 - \varepsilon) \right) \\
\left( t + \frac{1}{2} \right) / (1 - \varepsilon) &= (1 - \varepsilon - t) / (1 - \varepsilon) \\
t &= (1 - 2\varepsilon) / 4
\end{aligned}$$

so  $\text{CLMS}(F_\varepsilon)$  becomes

$$\begin{aligned}
\text{CLMS}(F_\varepsilon) &= \frac{1}{2} \left( F_\varepsilon^{-1} \left( (1 - 2\varepsilon) / 4 + \frac{1}{2} \right) - F_\varepsilon^{-1} \left( (1 - 2\varepsilon) / 4 \right) \right) \\
&= \frac{1}{2} \left( F^{-1} \left( (3 - 2\varepsilon) / (4(1 - \varepsilon)) \right) - F^{-1} \left( (1 - 2\varepsilon) / (4(1 - \varepsilon)) \right) \right).
\end{aligned}$$

Differentiation yields the influence function in this  $\theta$ :

$$\begin{aligned}
\text{IF}(\theta, \text{CLMS}, F) &= \frac{\partial}{\partial \varepsilon} \text{CLMS}(F_\varepsilon) \Big|_{\varepsilon=0+} \\
&= \frac{1}{2f(F^{-1}(3/4))} \frac{\partial}{\partial \varepsilon} \frac{3 - 2\varepsilon}{4(1 - \varepsilon)} \Big|_{\varepsilon=0+} \\
&\quad - \frac{1}{2f(F^{-1}(3/4))} \frac{\partial}{\partial \varepsilon} \frac{1 - 2\varepsilon}{4(1 - \varepsilon)} \Big|_{\varepsilon=0+} \\
&= \frac{1}{2f(F^{-1}(3/4))} \frac{\partial}{\partial \varepsilon} \frac{1}{2(1 - \varepsilon)} \Big|_{\varepsilon=0+} \\
&= \frac{1}{4f(F^{-1}(3/4))}.
\end{aligned}$$

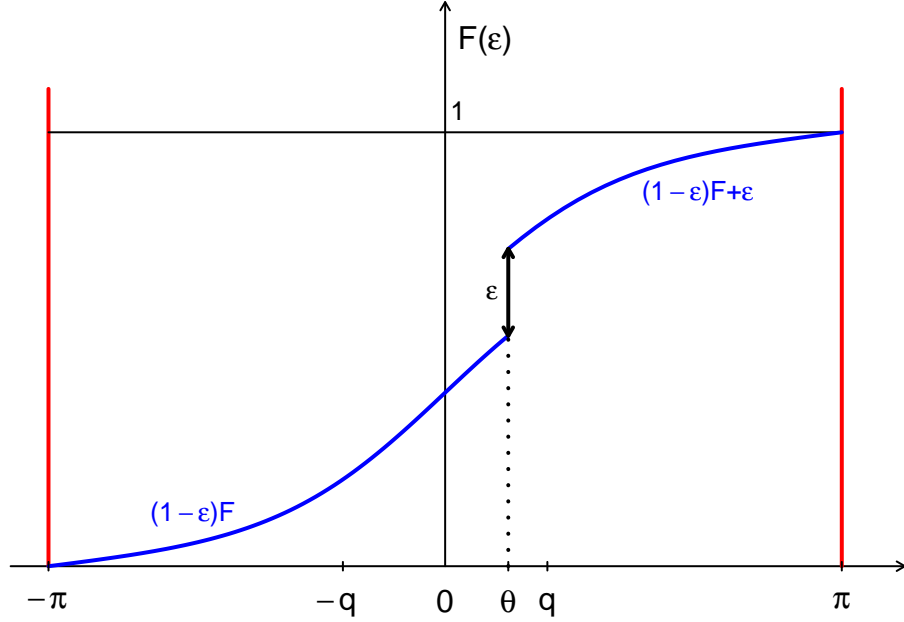


Figure S4: Sketch of the second part of the proof for CLMS, where  $-q < \theta < q$ .

We also have the situation where  $-q < \theta < q$  as sketched in Figure S4. The upper endpoint of the interval now lies in the region where  $F_\varepsilon(u) = (1 - \varepsilon)F(u) + \varepsilon$ , so minimizing (16) yields

$$\begin{aligned}
\frac{\partial}{\partial t} \frac{1}{2} \left( F_\varepsilon^{-1} \left( t + \frac{1}{2} \right) - F_\varepsilon^{-1}(t) \right) &= 0 \\
\frac{\partial}{\partial t} \left( F^{-1} \left( \frac{t + \frac{1}{2} - \varepsilon}{1 - \varepsilon} \right) - F^{-1} \left( \frac{t}{1 - \varepsilon} \right) \right) &= 0 \\
f \left( F^{-1} \left( \frac{t + \frac{1}{2} - \varepsilon}{1 - \varepsilon} \right) \right) &= f \left( F^{-1} \left( \frac{t}{1 - \varepsilon} \right) \right) \\
F^{-1} \left( \frac{t + \frac{1}{2} - \varepsilon}{1 - \varepsilon} \right) &= F^{-1} \left( 1 - \frac{t}{1 - \varepsilon} \right) \\
\frac{t + \frac{1}{2} - \varepsilon}{1 - \varepsilon} &= \frac{1 - \varepsilon - t}{1 - \varepsilon} \\
t &= 1/4
\end{aligned}$$

so  $\text{CLMS}(F_\varepsilon)$  becomes

$$\begin{aligned}
\text{CLMS}(F_\varepsilon) &= \frac{1}{2} \left( F_\varepsilon^{-1} \left( 3/4 \right) - F_\varepsilon^{-1} \left( 1/4 \right) \right) \\
&= \frac{1}{2} \left( F^{-1} \left( \frac{3/4 - \varepsilon}{1 - \varepsilon} \right) - F^{-1} \left( \frac{1/4}{1 - \varepsilon} \right) \right) \\
&= \frac{1}{2} \left( F^{-1} \left( \frac{3 - 4\varepsilon}{4(1 - \varepsilon)} \right) - F^{-1} \left( \frac{1}{4(1 - \varepsilon)} \right) \right).
\end{aligned}$$

Differentiation yields the influence function in this  $\theta$ :

$$\begin{aligned}
\text{IF}(\theta, \text{CLMS}, F) &= \left. \frac{\partial}{\partial \varepsilon} \text{CLMS}(F_\varepsilon) \right|_{\varepsilon=0+} \\
&= \left. \frac{1}{2f(F^{-1}(3/4))} \frac{\partial}{\partial \varepsilon} \frac{3-4\varepsilon}{4(1-\varepsilon)} \right|_{\varepsilon=0+} \\
&\quad - \left. \frac{1}{2f(F^{-1}(3/4))} \frac{\partial}{\partial \varepsilon} \frac{1}{4(1-\varepsilon)} \right|_{\varepsilon=0+} \\
&= \left. \frac{1}{2f(F^{-1}(3/4))} \frac{\partial}{\partial \varepsilon} \frac{1-2\varepsilon}{2(1-\varepsilon)} \right|_{\varepsilon=0+} \\
&= \frac{-1}{4f(F^{-1}(3/4))}.
\end{aligned}$$

This ends the proof.

**Proof of Theorem 7** We will use the property that the IF is symmetric because  $F$  is, that is,  $\text{IF}(-\theta, S, F) = \text{IF}(\theta, S, F)$ . Therefore we can compute the IF by contaminating  $F$  in a symmetric way, by putting  $F_\varepsilon := (1-\varepsilon)F + \frac{\varepsilon}{2}\Delta_\theta + \frac{\varepsilon}{2}\Delta_{-\theta}$  as illustrated in Figure S5. Now the cumulative distribution function  $F_\varepsilon$  is continuous on  $[-\pi, -\theta[$  where  $F_\varepsilon(u) = (1-\varepsilon)F(u)$ , then jumps up  $\frac{\varepsilon}{2}$  at  $-\theta$ , continues as  $(1-\varepsilon)F(u) + \frac{\varepsilon}{2}$ , jumps up again at  $\theta$ , and finally becomes  $(1-\varepsilon)F(u) + \varepsilon$ . As before  $F_\varepsilon(-\pi) = 0$  and  $F_\varepsilon(\pi) = 1$ .

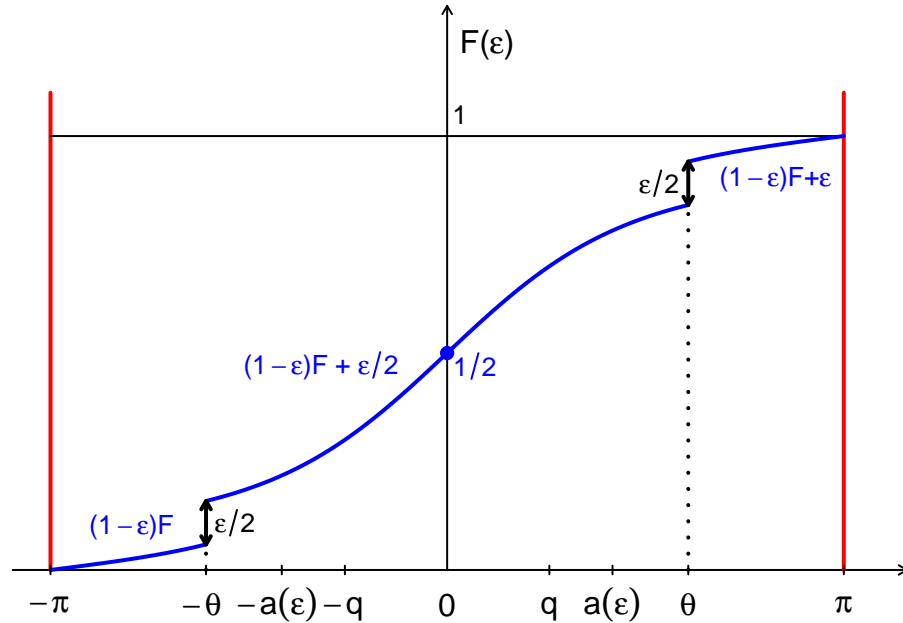


Figure S5: Sketch of the first part of the proof for CLTS, where  $q < \theta \leq \pi$ .

Let us start with the case where  $|\theta| > q$  where  $q = F^{-1}(3/4)$ . We can assume w.l.o.g. that  $\theta$  is positive, as in Figure S5. We will denote the interval of mass  $\frac{1}{2}$  and smallest circular variance by  $[-a(\varepsilon), a(\varepsilon)]$ . For small enough  $\varepsilon$  we have  $\theta > a(\varepsilon)$  because we know that  $\lim_{\varepsilon \downarrow 0} a(\varepsilon) = q < \theta$ . This implies that  $[-a(\varepsilon), a(\varepsilon)]$  lies entirely in the region where  $F_\varepsilon(u) = (1 - \varepsilon)F(u) + \frac{\varepsilon}{2}$  which yields

$$\begin{aligned} \frac{3}{4} &= F_\varepsilon(a(\varepsilon)) = (1 - \varepsilon)F(a(\varepsilon)) + \frac{\varepsilon}{2} \\ (1 - \varepsilon)F(a(\varepsilon)) &= \frac{3 - 2\varepsilon}{4} \\ a(\varepsilon) &= F^{-1}\left(\frac{3 - 2\varepsilon}{4 - 4\varepsilon}\right). \end{aligned}$$

Now  $S(F_\varepsilon)$  is given by the formula (10) with  $\phi_1 = -a(\varepsilon)$  and  $\phi_2 = a(\varepsilon)$ . By continuity of  $F_\varepsilon$  in these two points we know that  $P(-a(\varepsilon) \leq u \leq a(\varepsilon)) = \frac{1}{2}$  (and not strictly larger than  $\frac{1}{2}$ ). Therefore (10) becomes

$$\begin{aligned} S(F_\varepsilon) &= 2\sqrt{\int_{-a(\varepsilon)}^{a(\varepsilon)} (1 - \cos(u))dF_\varepsilon(u)} \\ &= 2\sqrt{0.5 - c(\varepsilon)} \end{aligned}$$

where  $c(\varepsilon)$  is the integral

$$c(\varepsilon) := \int_{-a(\varepsilon)}^{a(\varepsilon)} \cos(u)dF_\varepsilon(u) = (1 - \varepsilon) \int_{-a(\varepsilon)}^{a(\varepsilon)} \cos(u)f(u)du.$$

To obtain the IF we have to differentiate  $S(F_\varepsilon)$  with respect to  $\varepsilon = 0+$ , yielding

$$\begin{aligned} \frac{\partial S(F_\varepsilon)}{\partial \varepsilon} &= 2\frac{\partial}{\partial \varepsilon} \sqrt{0.5 - c(\varepsilon)} = \frac{2}{2\sqrt{0.5 - c(0)}} \frac{\partial}{\partial \varepsilon} (-c(\varepsilon)) \\ &= \frac{2}{S(F)} \left[ \int_{-a(0)}^{a(0)} \cos(u)f(u)du - \cos(a(0))f(a(0))\frac{\partial}{\partial \varepsilon} a(\varepsilon) \right. \\ &\quad \left. + \cos(-a(0))f(-a(0))\frac{\partial}{\partial \varepsilon} (-a(\varepsilon)) \right] \\ &= \frac{2}{S(F)} \left[ \int_{-q}^q \cos(u)f(u)du - 2\cos(q)f(q)\frac{\partial}{\partial \varepsilon} F^{-1}\left(\frac{3 - 2\varepsilon}{4 - 4\varepsilon}\right) \right] \\ &= \frac{2}{S(F)} \left[ c(0) - 2\cos(q)f(q)\frac{1}{f(F^{-1}(3/4))}\frac{\partial}{\partial \varepsilon} \left(\frac{3 - 2\varepsilon}{4 - 4\varepsilon}\right) \right] \\ &= \frac{2}{S(F)} \left[ \frac{1}{2} - \frac{S^2(F)}{4} - \frac{1}{2}\cos(F^{-1}(3/4)) \right] \\ &= \frac{1}{S(F)} \left[ 1 - \frac{S^2(F)}{2} - \cos(F^{-1}(3/4)) \right]. \end{aligned}$$

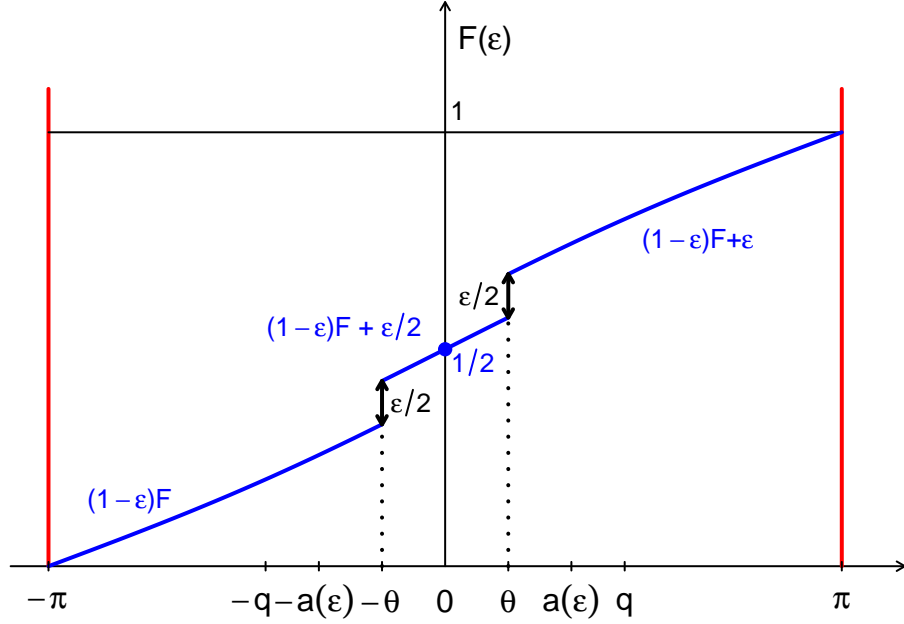


Figure S6: Sketch of the second part of the proof for CLTS, where  $-q < \theta < q$ .

We now switch to the case where  $|\theta| < q$  as illustrated in Figure S6. For small enough  $\varepsilon$  we have  $\theta < a(\varepsilon)$  because  $y < q = \lim_{\varepsilon \downarrow 0} a(\varepsilon)$ . Therefore both upward jumps of  $F_\varepsilon$  occur inside  $[-a(\varepsilon), a(\varepsilon)]$ , so this time

$$\begin{aligned} \frac{3}{4} &= F_\varepsilon(a(\varepsilon)) = (1 - \varepsilon)F(a(\varepsilon)) + \varepsilon \\ (1 - \varepsilon)F(a(\varepsilon)) &= \frac{3 - 4\varepsilon}{4} \\ a(\varepsilon) &= F^{-1}\left(\frac{3 - 4\varepsilon}{4 - 4\varepsilon}\right). \end{aligned}$$

Also here  $S(F_\varepsilon)$  is twice the square root of the circular variance on  $[-a(\varepsilon), a(\varepsilon)]$ , but the expressions become a bit longer since the point masses in  $-\theta$  and  $\theta$  occur inside the interval, so now

$$\begin{aligned} c(\varepsilon) &= \int_{-a(\varepsilon)}^{a(\varepsilon)} \cos(u) dF_\varepsilon(u) \\ &= (1 - \varepsilon) \int_{-a(\varepsilon)}^{a(\varepsilon)} \cos(u) dF(u) + \frac{\varepsilon}{2} \cos(\theta) + \frac{\varepsilon}{2} \cos(-\theta) \\ &= (1 - \varepsilon) \int_{-a(\varepsilon)}^{a(\varepsilon)} \cos(u) dF(u) + \varepsilon \cos(\theta). \end{aligned}$$

This time we obtain

$$\begin{aligned}
\frac{\partial S(F_\varepsilon)}{\partial \varepsilon} &= \frac{\partial}{\partial \varepsilon} 2\sqrt{0.5 - c(\varepsilon)} = \frac{2}{2\sqrt{0.5 - c(0)}} \frac{\partial}{\partial \varepsilon} (-c(\varepsilon)) \\
&= \frac{2}{S(F)} \left[ \int_{-a(0)}^{a(0)} \cos(u)f(u)du - \cos(a(0))f(a(0))\frac{\partial}{\partial \varepsilon} a(\varepsilon) \right. \\
&\quad \left. + \cos(-a(0))f(-a(0))\frac{\partial}{\partial \varepsilon} (-a(\varepsilon)) - \frac{1}{2}\cos(\theta) - \frac{1}{2}\cos(-\theta) \right] \\
&= \frac{2}{S(F)} \left[ \int_{-q}^q \cos(u)f(u)du - 2\cos(q)f(q)\frac{\partial}{\partial \varepsilon} F^{-1}\left(\frac{3-4\varepsilon}{4-4\varepsilon}\right) - \cos(\theta) \right] \\
&= \frac{2}{S(F)} \left[ c(0) - 2\cos(q)f(q)\frac{1}{f(F^{-1}(3/4))}\frac{\partial}{\partial \varepsilon} \left(\frac{3-4\varepsilon}{4-4\varepsilon}\right) - \cos(\theta) \right] \\
&= \frac{2}{S(F)} \left[ \frac{1}{2} - \frac{S^2(F)}{4} + \frac{1}{2}\cos(F^{-1}(3/4)) - \cos(\theta) \right] \\
&= \frac{1}{S(F)} \left[ 1 - \frac{S^2(F)}{2} + \cos(F^{-1}(3/4)) - 2\cos(\theta) \right].
\end{aligned}$$

Combining the results for  $|\theta| > q$  and  $|\theta| < q$  yields the statement of the theorem.

## C: Breakdown values

**Proof of Lemma 6.** We first show that a distribution  $H^*$  exists such that the breakdown value is exactly equal to the right-hand expression in Equation (21). Then, we show there exists a second distribution  $H^{**}$  where the breakdown value is lower, although not derivable in a closed form.

Consider the distribution  $G^* := (1 - \varepsilon)F + \varepsilon H^*$ , where  $H^* := 0.5\Delta_{\mu-\pi/2} + 0.5\Delta_{\mu+\pi/2}$ . Note that, by the symmetry of  $H^*$  with respect to  $\mu$ , and because  $F$  has a unique mode in  $\mu$  and density monotonically decreasing from  $\mu$  to  $\mu \pm \pi$ , we have that the median of  $G^*$  is unique and equals the median of  $F$ :  $\tilde{\mu}_{G^*} = \tilde{\mu}_F = \mu$ .

Consider the values of  $\varepsilon$  for which  $\text{CMAD}(G^*) = \pi/2$ . By definition of CMAD (Equation 5),  $\text{CMAD}(G^*) = \pi/2$  if

$$P_{G^*}(\mu - \pi/2 < \theta < \mu + \pi/2) < 0.5 \tag{29}$$

and if

$$P_{G^*}(\mu - \pi/2 \leq \theta \leq \mu + \pi/2) \geq 0.5, \tag{30}$$

where the first condition ensures that there is no arc shorter than  $\pi/2$  with probability content at least 0.5 under  $G^*$ .

The second condition is always satisfied. Given that both  $P_F(\mu - \pi/2 \leq \theta \leq \mu + \pi/2) \geq 0.5$  and  $P_{H^*}(\mu - \pi/2 \leq \theta \leq \mu + \pi/2) \geq 0.5$ , any linear combination of them is also  $\geq 0.5$ . Hence (30) is satisfied for any  $\varepsilon \leq 0.5$ .

For the first condition to be satisfied, a constraint applies. First note that, by definition of  $H^*$ ,  $P_{H^*}(\mu - \pi/2 < \Theta < \mu + \pi/2) = 0$ , and thus

$$P_{G^*}(\mu - \pi/2 < \Theta < \mu + \pi/2) = (1 - \varepsilon)P_F(\mu - \pi/2 < \Theta < \mu + \pi/2) \quad \forall \varepsilon.$$

Hence, condition (29) becomes

$$(1 - \varepsilon)P_F(\mu - \pi/2 < \Theta < \mu + \pi/2) < 0.5,$$

which is satisfied if  $\varepsilon > 1 - 0.5[P_F(\mu - \pi/2 < \Theta < \mu + \pi/2)]^{-1}$ , so that

$$\inf\{\varepsilon : \text{CMAD}(G^*) = \pi/2\} = 1 - 0.5[P_F(\mu - \pi/2 < \Theta < \mu + \pi/2)]^{-1}.$$

To complete the proof, we need to show that at least one distribution  $H^{**}$  exists such that  $\inf\{\varepsilon : \text{CMAD}(G^{**}) = \pi/2\} < \inf\{\varepsilon : \text{CMAD}(G^*) = \pi/2\}$ , where  $G^{**} := (1 - \varepsilon)F + \varepsilon H^{**}$  (if not, then (21) would not describe an upper limit but the breakdown value itself).

Let  $H^{**} := (1 - \alpha)\Delta_{\tilde{\mu}_{G^{**}} - \pi/2} + \alpha\Delta_{\tilde{\mu}_{G^{**}} + \pi/2}$ ,  $0 \leq \alpha \leq 1$ ,  $\alpha \neq 0.5$ . If so, then  $G^{**}$  is an asymmetric distribution, and  $\tilde{\mu}_{G^{**}} \neq \tilde{\mu}_F$ , where the position of  $\tilde{\mu}_{G^{**}}$  on the circle depends on the value of  $\alpha$ , and, most importantly, on the value of  $\varepsilon$  itself. As a consequence, no closed form can be derived to obtain the value of  $\tilde{\mu}_{G^{**}}$ .

On the other hand,  $\tilde{\mu}_{G^{**}} \in [\mu - \pi/2, \mu + \pi/2]$ . First, note that  $\tilde{\mu}_{G^{**}}$  cannot be antipodal to  $\mu$  for any value of  $\varepsilon$  and  $\psi$ , because  $\alpha \neq 0.5$ . In addition, if  $\alpha < 0.5$ , then  $\tilde{\mu}_{G^{**}} \in [\mu - \pi/2, \mu] \forall \varepsilon, \psi$ , and vice versa.

Eventually, to get  $\text{CMAD}(G^{**}) = \pi/2$ , and hence to break down  $\hat{\psi}_{\text{CMAD}}$ , in analogy with conditions (29) and (30), we must have

$$P_{G^{**}}(\tilde{\mu}_{G^{**}} - \pi/2 < \Theta < \tilde{\mu}_{G^{**}} + \pi/2) < 0.5 \tag{31}$$

and

$$P_{G^{**}}(\tilde{\mu}_{G^{**}} - \pi/2 \leq \Theta \leq \tilde{\mu}_{G^{**}} + \pi/2) \geq 0.5. \tag{32}$$

The second condition is always satisfied, given that both  $P_F(\tilde{\mu}_{G^{**}} - \pi/2 \leq \theta \leq \tilde{\mu}_{G^{**}} + \pi/2) \geq 0.5$ , and  $P_{H^{**}}(\tilde{\mu}_{G^{**}} - \pi/2 \leq \Theta \leq \tilde{\mu}_{G^{**}} + \pi/2) \geq 0.5$ , where the first holds because  $\tilde{\mu}_{G^{**}} \in [\mu - \pi/2, \mu + \pi/2]$  and  $F$  has  $\geq 0.5$  probability for each semicircle that contains  $\mu$ .

For the first condition to be satisfied, because  $P_{G^{**}}(\tilde{\mu}_{G^{**}} - \pi/2 < \Theta < \tilde{\mu}_{G^{**}} + \pi/2) = (1 - \varepsilon)P_F(\tilde{\mu}_{G^{**}} - \pi/2 < \Theta < \tilde{\mu}_{G^{**}} + \pi/2)$  by definition of  $H^{**}$ , we need  $(1 - \varepsilon)P_F(\tilde{\mu}_{G^{**}} - \pi/2 < \Theta < \tilde{\mu}_{G^{**}} + \pi/2) < 0.5$  which is in turn satisfied for  $\varepsilon > 1 - 0.5[P_F(\tilde{\mu}_{G^{**}} - \pi/2 < \Theta < \tilde{\mu}_{G^{**}} + \pi/2)]^{-1}$ , so that

$$\inf\{\varepsilon : \text{CMAD}(G^{**}) = \pi/2\} = 1 - 0.5[P_F(\tilde{\mu}_{G^{**}} - \pi/2 < \Theta < \tilde{\mu}_{G^{**}} + \pi/2)]^{-1}.$$

The proof is completed, as  $\inf\{\varepsilon : \text{CMAD}(G^{**}) = \pi/2\} < \inf\{\varepsilon : \text{CMAD}(G^*) = \pi/2\}$  given that  $P_F(\mu - \pi/2 < \Theta < \mu + \pi/2) > P_F(\tilde{\mu}_{G^{**}} - \pi/2 < \Theta < \tilde{\mu}_{G^{**}} + \pi/2)$ , because  $\tilde{\mu}_{G^{**}} \neq \mu$ .

For both the von Mises and the wrapped normal distributions,  $P_F(\mu - \pi/2 < \Theta < \mu + \pi/2) > 0.5 \forall \psi > 0$ . Hence, the upper bound given in (21) is always less than 0.5.

**Proof of Theorem 8.** By definition of the explosion breakdown value,  $\varepsilon_{\text{exp}}^*(\widehat{\psi}_{\text{CMAD}}) = \inf\{\varepsilon : \text{CMAD}((1 - \varepsilon)F + \varepsilon H) = 0\}$ . By the continuity of  $\Theta$ , and because of Lemma 1,  $\text{CMAD}((1 - \varepsilon)F + \varepsilon H) = 0$  only if  $H = \Delta_\theta$  for some  $\theta$ , and  $\varepsilon \geq 0.5$ . The result follows.

## D: Asymptotic variances and relative efficiencies

In this section we study the asymptotic behavior of the robust dispersion functionals CMAD, CLMS, and CLTS at a parametric circular model. In a given model, the functional is transformed to become Fisher consistent for a specific parameter, here the  $\kappa$  of the von Mises model and the  $\sigma$  of the wrapped normal. We will derive the asymptotic variance of the transformed functional from that of the original functional.

In the following theorems we compute the asymptotic variance of the functionals CMAD, CLMS, CLTS, and their derived estimators.

**Theorem 11** (Asymptotic variance of CMAD and CLMS.). *Let  $F$  be a circular distribution with continuous density  $f(\theta) > 0$ . Let  $S(F)$  denote the CMAD or the CLMS functional and let  $S_n = S(F_n)$  be its sample version based on the empirical distribution  $F_n$ . The influence function of  $S$  is given by Theorem 6, and the asymptotic variance of the estimator  $S_n$  equals*

$$\text{AVar}(S_n) = \frac{1}{16 f(F^{-1}(3/4))^2}.$$

*Proof* The asymptotic variance of an estimator  $S_n$  is given by

$$\text{AVar}(S_n) = \mathbb{E}_F[\text{IF}(\theta; S, F)^2],$$

where  $\text{IF}(\theta; S, F)$  is the influence function of  $S$  at  $F$ . For CMAD or CLMS, the influence function is

$$\text{IF}(\theta; S, F) = \frac{\text{sign}(|\theta| - F^{-1}(3/4))}{4 f(F^{-1}(3/4))}.$$

Squaring and taking expectation gives

$$\mathbb{E}_F[\text{IF}^2] = \int_{-\pi}^{\pi} \left( \frac{\text{sign}(|\theta| - F^{-1}(3/4))}{4 f(F^{-1}(3/4))} \right)^2 f(\theta) d\theta = \int_{-\pi}^{\pi} \frac{1}{16 f(F^{-1}(3/4))^2} f(\theta) d\theta.$$

Since  $\int_{-\pi}^{\pi} f(\theta) d\theta = 1$ , we obtain

$$\text{AVar}(S_n) = \frac{1}{16 f(F^{-1}(3/4))^2}.$$

**Theorem 12** (Asymptotic variance of CLTS.). *Let  $F$  be a circular distribution with continuous density  $f(\theta) > 0$  that is symmetric and strictly unimodal with mode 0. Let  $S(F)$  denote the CLTS functional and let  $S_n = S(F_n)$  be its sample version based on the empirical distribution  $F_n$ . The influence function of  $S$  is given by Theorem 7, and the asymptotic variance of  $S_n$  equals*

$$\begin{aligned} \text{AVar}(S_n) &= \frac{1}{S^2(F)} \left[ \left( 1 - \frac{S^2(F)}{2} - \cos(F^{-1}(3/4)) \right)^2 \right. \\ &\quad + 4 \left( 1 - \frac{S^2(F)}{2} - \cos(F^{-1}(3/4)) \right) \int_{F^{-1}(1/4)}^{F^{-1}(3/4)} (\cos(F^{-1}(3/4)) - \cos \theta) dF(\theta) \\ &\quad \left. + 4 \int_{F^{-1}(1/4)}^{F^{-1}(3/4)} (\cos(F^{-1}(3/4)) - \cos \theta)^2 dF(\theta) \right]. \end{aligned}$$

*Proof* The influence function of  $S$  is

$$\text{IF}(\theta; S, F) = \frac{1}{S(F)} \left[ 1 - \frac{S^2(F)}{2} - \cos(F^{-1}(3/4)) + 2 I(|\theta| < F^{-1}(3/4)) (\cos(F^{-1}(3/4)) - \cos \theta) \right],$$

so the asymptotic variance equals

$$\begin{aligned} \text{AVar}(S_n) &= \mathbb{E}_F [\text{IF}(\theta; S, F)^2] \\ &= \frac{1}{S^2(F)} \mathbb{E}_F \left[ \left( 1 - \frac{S^2(F)}{2} - \cos F^{-1}(3/4) \right. \right. \\ &\quad \left. \left. + 2 I(|\theta| < F^{-1}(3/4)) (\cos F^{-1}(3/4) - \cos \theta) \right)^2 \right]. \end{aligned}$$

Expanding the square and using  $F^{-1}(1/4) = -F^{-1}(3/4)$  allows the integrals to be written as

$$\begin{aligned} \text{AVar}(S_n) &= \frac{1}{S^2(F)} \left[ \left( 1 - \frac{S^2(F)}{2} - \cos(F^{-1}(3/4)) \right)^2 \right. \\ &\quad + 4 \left( 1 - \frac{S^2(F)}{2} - \cos F^{-1}(3/4) \right) \int_{F^{-1}(1/4)}^{F^{-1}(3/4)} (\cos F^{-1}(3/4) - \cos \theta) dF(\theta) \\ &\quad \left. + 4 \int_{F^{-1}(1/4)}^{F^{-1}(3/4)} (\cos F^{-1}(3/4) - \cos \theta)^2 dF(\theta) \right]. \end{aligned}$$

**Theorem 13** (Asymptotic variance of the transformed estimators.). *Let  $S$  denote the CMAD, CLMS or CLTS functional and let  $\psi_S = \zeta(S)$  be its corresponding transformation. Let  $S_n = S(F_n)$  and  $\widehat{\psi}_S = \zeta(S_n)$  be the corresponding estimator based on the empirical distribution  $F_n$ . If  $\zeta$  is continuously differentiable at  $S(F)$ , then the asymptotic variance of  $\widehat{\psi}$  equals*

$$\text{AVar}(\widehat{\psi}_S) = \left( \zeta'(S(F)) \right)^2 \text{AVar}(S_n).$$

*Proof.* The influence function of  $\psi_S$  is given by

$$\text{IF}(x; \psi_S, F) = \zeta'(S(F)) \text{IF}(x; S, F).$$

Substitution into the asymptotic variance formula

$$\text{AVar}(\widehat{\psi}_S) = \int \text{IF}(x; \psi_S, F)^2 dF(x)$$

yields the stated result. □

**Theorem 14** (Asymptotic variance of  $\widehat{\kappa}$  at the von Mises distribution.). *Let  $F$  be a von Mises distribution with concentration parameter  $\kappa$ , and let CSD be its population circular standard deviation that is related to  $\kappa$  by*

$$\kappa = g(\text{CSD}) = A^{-1}\left(1 - \frac{\text{CSD}^2}{2}\right).$$

*Let  $S_n$  be an estimator of CSD and define the induced estimator of  $\kappa$  by  $\widehat{\kappa} = g(S_n)$ . Then the asymptotic variance of  $\widehat{\kappa}$  equals*

$$\text{AVar}(\widehat{\kappa}) = \frac{\text{CSD}^2}{A'(\kappa)^2} \text{AVar}(S). \quad (33)$$

*Proof* For the von Mises distribution

$$\rho = A(\kappa) = \frac{I_1(\kappa)}{I_0(\kappa)} \quad \text{and} \quad \text{CSD} = \sqrt{2(1 - \rho)},$$

so  $\rho = 1 - \text{CSD}^2/2$ . Solving for  $\kappa$  as a function of CSD, we obtain

$$\kappa = A^{-1}\left(1 - \frac{\text{CSD}^2}{2}\right).$$

We now define the function  $g$  by  $g(S) := A^{-1}(1 - S^2/2)$ , so that  $\kappa = g(S)$  and  $\widehat{\kappa} = g(S_n)$ . Since  $A(\kappa)$  is continuously differentiable and strictly increasing, the function  $g$  is differentiable at CSD with derivative

$$g'(S) = \frac{d}{dR} A^{-1}(R) \Big|_{R=A(\kappa)} \frac{d}{dS} \left(1 - \frac{S^2}{2}\right).$$

Since

$$\frac{d}{dR} A^{-1}(R) \Big|_{R=A(\kappa)} = \frac{1}{A'(\kappa)} \quad \text{and} \quad \frac{d}{dS} \left(1 - \frac{S^2}{2}\right) = -S,$$

we obtain

$$g'(S(F)) = -\frac{S(F)}{A'(\kappa)} = -\frac{\text{CSD}}{A'(\kappa)}.$$

We know that

$$\text{AVar}(\widehat{\kappa}) = (g'(S(F)))^2 \text{AVar}(S_n).$$

Therefore, the asymptotic variance of  $\widehat{\kappa}$  is indeed

$$\text{AVar}(\widehat{\kappa}) = \frac{\text{CSD}^2}{(A'(\kappa))^2} \text{AVar}(S_n).$$

**Theorem 15** (Asymptotic variance of  $\hat{\sigma}$  at the wrapped normal.). *Let  $F$  be a wrapped normal distribution with scale parameter  $\sigma$  and let CSD denote the circular standard deviation, that is related to  $\sigma$  by*

$$\sigma = g(\text{CSD}) = \sqrt{-2 \log \left( 1 - \frac{\text{CSD}^2}{2} \right)}.$$

*Let  $S_n$  be an estimator of CSD and define the induced estimator of  $\sigma$  by  $\hat{\sigma} = g(S_n)$ . Then the asymptotic variance  $\text{AVar}(\hat{\sigma})$  equals*

$$\text{AVar}(\hat{\sigma}) = \frac{\text{CSD}^2}{\sigma^2 \left( 1 - \frac{\text{CSD}^2}{2} \right)^2} \text{AVar}(S_n). \quad (34)$$

*Proof* For the wrapped normal distribution, the mean resultant length is

$$\rho = e^{-\sigma^2/2}.$$

Since  $\rho$  is connected to CSD by  $\text{CSD} = \sqrt{2(1-\rho)}$  we have  $\rho = 1 - \text{CSD}^2/2$ . This yields

$$e^{-\sigma^2/2} = 1 - \frac{\text{CSD}^2}{2}.$$

Solving for  $\sigma$  yields

$$\sigma = \sqrt{-2 \log \left( 1 - \frac{\text{CSD}^2}{2} \right)}.$$

We now define the function  $g$  by

$$g(S) := \sqrt{-2 \log \left( 1 - \frac{S^2}{2} \right)},$$

so that  $\sigma = g(S)$  and  $\hat{\sigma} = g(S_n)$ . The function  $g$  is continuously differentiable at CSD with derivative

$$g'(S) = \frac{d}{d\rho} \left( \sqrt{-2 \log \rho} \right) \Big|_{\rho=1-\frac{S^2}{2}} \frac{d}{dS} \left( 1 - \frac{S^2}{2} \right).$$

Since

$$\frac{d}{d\rho} \left( \sqrt{-2 \log \rho} \right) = -\frac{1}{\rho \sqrt{-2 \log \rho}} \quad \text{and} \quad \frac{d}{dS} \left( 1 - \frac{S^2}{2} \right) = -S,$$

we obtain, using  $\rho = 1 - \frac{S^2}{2}$  and  $\sigma = \sqrt{-2 \log \rho}$ ,

$$g'(S) = \frac{S}{\sigma \left( 1 - \frac{S^2}{2} \right)}.$$

Because we know that

$$\text{AVar}(\hat{\sigma}) = ((\eta^{-1})'(S(F)))^2 \text{AVar}(S_n),$$

the asymptotic variance of  $\hat{\sigma}$  indeed equals

$$\text{AVar}(\hat{\sigma}) = \frac{\text{CSD}^2}{\sigma^2 \left(1 - \frac{\text{CSD}^2}{2}\right)^2} \text{AVar}(S_n).$$

### Efficiencies of $\hat{\psi}_{\text{CMAD}}$ , $\hat{\psi}_{\text{CLMS}}$ , $\hat{\psi}_{\text{CLTS}}$

The efficiency of the proposed robust estimators is assessed through their asymptotic relative efficiency (ARE) with respect to the maximum likelihood estimator (MLE) under the assumed model. For a parameter of interest  $\psi$  (e.g.,  $\kappa$  for the von Mises distribution or  $\sigma$  for the wrapped normal distribution), the ARE of an estimator  $\hat{\psi}$  is defined as

$$\text{ARE}(\hat{\psi}) = \frac{\text{AVar}(\hat{\psi}_{\text{MLE}})}{\text{AVar}(\hat{\psi})}.$$

For the von Mises distribution, the maximum likelihood estimator  $\hat{\kappa}_{\text{MLE}}$  of the concentration parameter  $\kappa$  is asymptotically normal with variance

$$\text{AVar}(\hat{\kappa}_{\text{MLE}}) = \frac{1}{I(\kappa)},$$

where the Fisher information is given by

$$I(\kappa) = \frac{1}{2} \left(1 + \frac{I_2(\kappa)}{I_0(\kappa)}\right) - \left(\frac{I_1(\kappa)}{I_0(\kappa)}\right)^2,$$

with  $I_0(\cdot)$ ,  $I_1(\cdot)$ , and  $I_2(\cdot)$  denoting the modified Bessel functions of the first kind of orders 0, 1, and 2.

Under the wrapped normal model with known  $\mu$ , the maximum likelihood estimator of the scale parameter  $\sigma$  is also asymptotically normal. Specifically,

$$\sqrt{n}(\hat{\sigma}_{\text{MLE}} - \sigma) \xrightarrow{d} \mathcal{N}(0, I(\sigma)^{-1}),$$

where  $I(\sigma)$  denotes the Fisher information that can be computed numerically.